UiT
THE ARCTIC
UNIVERSITY
OF NORWAY

Faculty of Biosciences, Fisheries and Economics

Department of Arctic and Marine Biology

The Marine Plastic Microbiome: *Microbial Colonization of Polymer Surfaces in the Arctic Marine Environment*

Tara M. Stitzlein

BIO-3950 Master's thesis in Biology, September 2018.

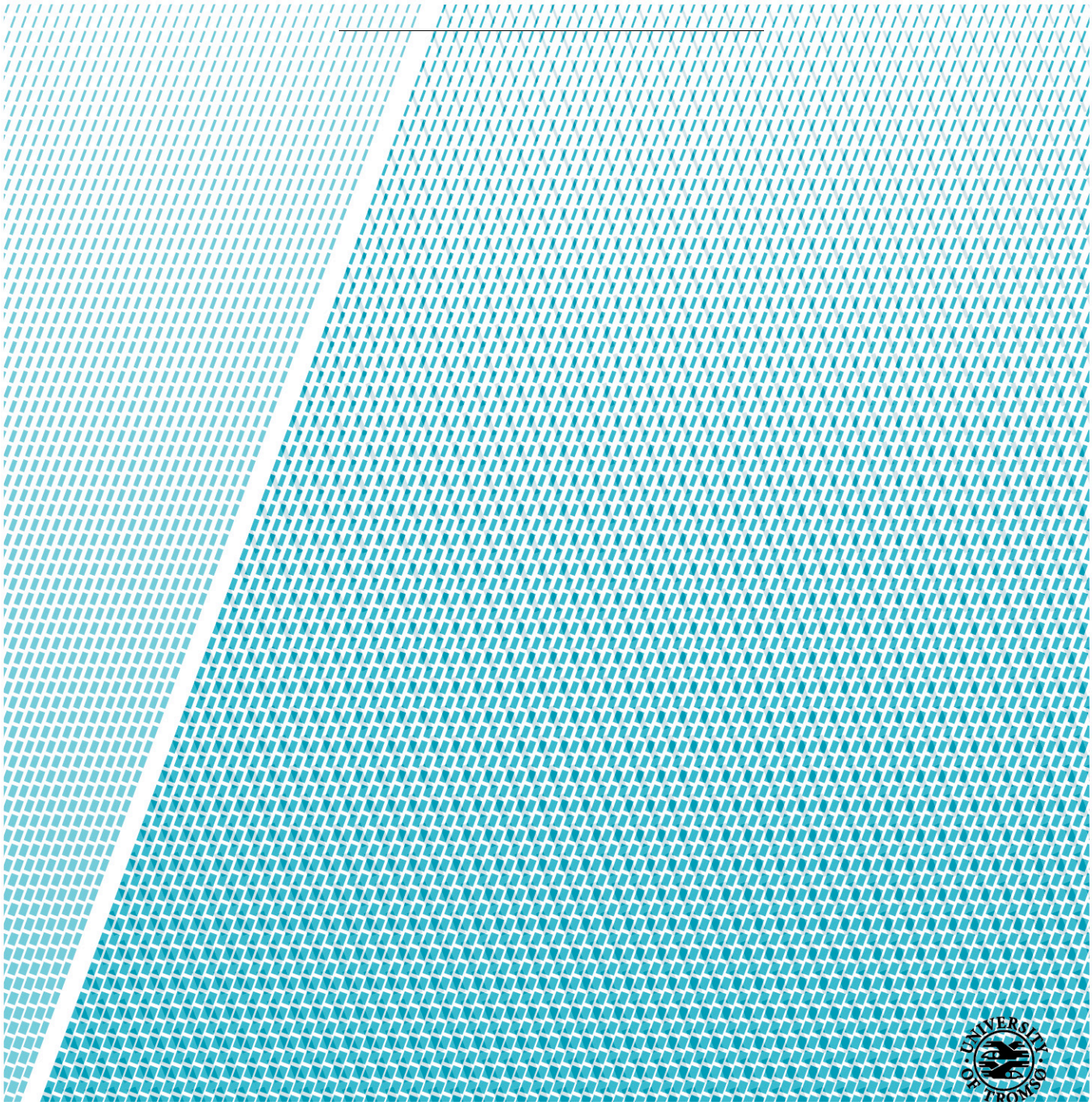

Supervisors:

Sophie Bourgeon (The Arctic University of Norway, UiT)

Dorte Herzke (Norwegian Institute for Air Research, NILU)

Geir Wing Gabrielsen (Norwegian Polar Institute, NPI)

Additional contributors:

Elena Sánchez Romeo (UiT)

Mette Marianne Svenning (UiT)

Alena Didriksen (UiT)

Tom-Ivar Eilertsen (UiT)

Augusta Hlin Aspar (UiT)

Funding and support:

Northern Environmental Waste Management (EWMA)

JPI Oceans (PLASTOX)

Acknowledgements

I would like to take this opportunity to thank the many organizations and people whose collective efforts have made this project possible.

Thank you primarily to my supervisors, Sophie Bourgeon, Dorte Herzke and Geir Wing-Gabrielson for your guidance and assistance with developing this project from its very beginnings. Thank you for your willingness to shape an ambitious idea into a manageable two-year project. Thank you to Dorte, NILU and the JPI Oceans PLASTOX project for the use of your materials and set-up for the field portion of this experiment. Thank you to Sophie for your many introductions, the use of your lab space, and your last-minute editing help. Thank you to Geir for your expertise and enthusiasm about the field of marine plastics.

Thank you to the Arctic University of Norway for the opportunity to undertake this project as my master's thesis. Special thanks to the Molecular Environmental Biology laboratory at UiT, Mette Marianne Svenning and Alena Didriksen for the use of your lab facilities and assistance in the lab. Thank you to the microscopy team of Tom-Ivar Eilertsen and Augusta Hlin Aspar at UiT for your assistance with preparing and imaging my samples. Also thanks to the UiT kayak club and Morgan Bender for allowing me the use of your boat ramp as a sampling location.

A big thank you to Elena Sánchez Romeo for your help in the lab and your assistance in developing a working protocol.

And finally, thanks to Cole and the many friends who assisted in various supportive roles including sewing clinicians, kayak crew members, international sample couriers and remote office accessors.

Abstract

While the sources and fates of plastic pollution are receiving growing attention, major knowledge gaps exist. Among these, microbial degradation (aka biodegradation) of plastics remains poorly investigated. The process of biodegradation begins with the formation of biofilm on the polymer surface; our study aimed to investigate microbial colonization of polymer surfaces in the Arctic marine environment around Tromsø, Norway. An immersion experiment was designed to assess microbiome community composition on four different types of pre-production microplastic (<5mm in diameter) pellets (Low-density polyethylene (LDPE), polypropylene (PP), polystyrene (PS) and polyethylene-terephthalate (PET)) and rubber (a non-synthetic polymer used as a control) over a period of 6 months at two different locations around Tromsø. Surface states of pre and post-immersion polymer samples were examined using Scanning Electron Microscopy. Samples were taken at 6 months post-immersion, and surface biofilm was subject to chemical and enzymatic digestion and DNA extraction by phenol-chloroform separation. Genotyping using 16S, 18S and ITS 2 rRNA gene amplification and next-generation sequencing on the Illumina platform was employed to identify bacterial, eukaryotic and fungal microbial life on the polymer surfaces. Investigation of the species richness and diversity within and among polymer types (alpha and beta-diversity, respectively) contribute key insights to the body of knowledge relating to the plastic microbiome and its potential role in polymer degradation. Taxonomic profiles were compared against a database of known polymer-degrading microbes to determine if any microbial degradation was likely under Arctic conditions. Several notable operational taxonomical units were identified including members belonging to obligate hydrocarbon-degrading bacterial species, marine fish pathogens, and members of families containing polymer-degrading bacterial species. Significant differences in community structure were noted between polymer-associated and both rubber and free-floating bacterial communities, as well as differences in select eukaryotic and fungal communities.

Table of Contents

Introduction

Origins and Applications of Plastics

In just over 100 years, plastics have grown from their infancy to become a global presence, both industrially and geographically. The demand for raw polymers has increased from 1.7 million tons in 1950 (Worldwatch Institute, 2015), to an estimated 335 million metric tons produced in 2016 (PlasticsEurope, 2017), with this trend expected to continue in the coming decades. As the field of polymer engineering has progressed, driven by the demand for more and better materials, plastics have evolved to fill emerging market niches, and to replace more conventional materials like wood, metal and glass.

The term plastic, often used interchangeably with polymer, actually describes a group of synthetic polymers, typically derived from natural gas, crude oil or coal (ACC). The manufacturing process begins with the separation and purification of hydrocarbons from the source material, which are then further processed to synthesize the real building blocks of plastics, double-bonded carbon atoms called monomers (ACC). Monomers are chemically joined by addition or condensation reactions to form long chains, resulting in the high molecular weight carbon chains we know as plastics (ACC). Varying the type and combination of monomers used will result in different degrees of material properties like strength, flexibility, chemical and heat resistance, and weight. Names and structures of some commonly used consumer plastics are included below in **Figure 1**.

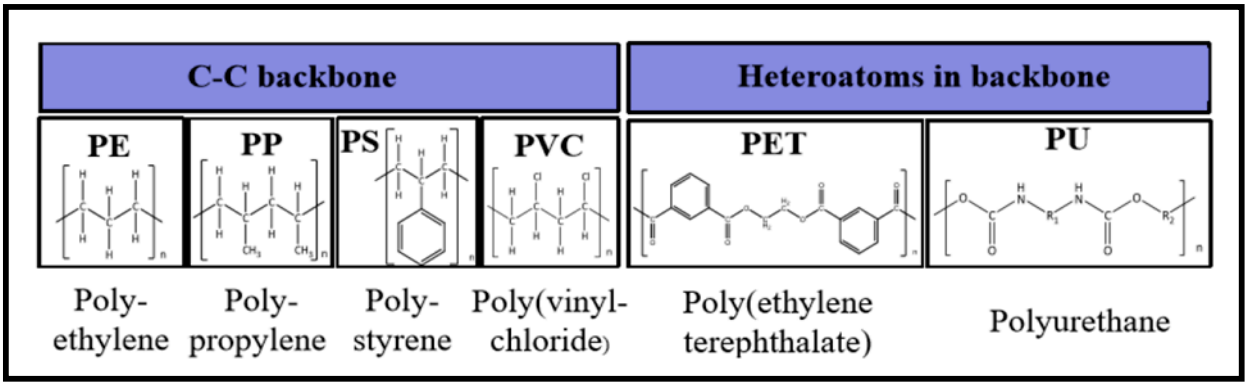

Figure 1. Molecular structures of various common synthetic polymers. Adapted from Gewart et al., 2015.

The array of potential characteristics that plastic can embody has made it an indispensable material, garnering widespread use across almost every industrial sector. According to the PlasticsEurope Market Research and Statistics Group, the packaging industry accounted for 40% of plastic demand in Europe in 2016; this was followed by building and construction (20%), automotive (10%), electronics (6%), household goods (4%), agriculture (3%), and "other" (17%) (PlasticsEurope 2017). The diverse nature of these industries illustrates the pivotal role plastic has played in shaping the anthropologic world since its inception. Inexpensive and versatile, durable yet light-weight, flexible but strong; plastic has changed the way we eat, the way we sleep and the way we work.

Figure 2. Plastic usage by type in the European market in 2017. Figure adapted from PlasticsEurope, Plastics – the Facts 2017 report.

Another key property of plastics is their ability to be repurposed for a second generation of use. When thermoplastics are recycled, high temperatures are used to melt the polymers down to be reformed. However, this thermal process is energy intensive, and often causes the polymer to lose some of its integrity. The resulting material is typically of a lower quality, making it difficult to use recycled plastic for its original purpose. Continued production of raw polymers is needed to provide the high-quality plastic that industry and consumers prefer, leading to the devaluation of plastic waste and resulting in a low profit margin for recycling facilities. Combined with the new cultural norm of single-use plastic, the end result is an increase in production, and a lagging global plastic recycling rate of less than 14% (World Economic Forum, 2016).

Marine Plastic Debris: Sources and Distribution

As the niche of the plastics market has expanded, so too has the magnitude and distribution of plastic waste. The relatively inexpensive manufacturing costs, rise in global consumption, and the emergence of a "throw-away" culture have led in quick succession to an overwhelming problem. Terrestrial landfills are ill-equipped, recycling facilities are grappling with the profitability and feasibility of returning these recalcitrant materials to a useable state, and up to 12 million metric tons of plastic debris are entering the world's oceans every year (Jambeck et al., 2015).

Occurrence of plastic debris in the oceans is well-documented and ubiquitous. It has been observed in remote and diverse areas: washed up on South-Pacific islands (Lavers & Bond, 2017), embedded in Arctic sea ice (Peeken et al, 2018), and isolated from the tissues of blue mussels on the French Atlantic coast (Phuong et al, 2018). Though prevalence of plastic debris is often higher near coastal areas with high human population density, the distribution of plastic throughout the world's ocean is more widespread than can be explained by proximity. As a steady stream of plastic has entered the oceans over the last few decades, global ocean currents have distributed marine plastic debris around the world, concentrating large masses in five accumulation zones, or "garbage patches", around the subtropical ocean gyres (Cózar et al, 2014). The Arctic Ocean has recently been characterized as a sort of dead-end for plastic debris, with a previously undocumented gyre forming in the Barents Sea (Cózar et al., 2017).

Marine plastic debris can be broadly classified based on its source: land-based sources and ocean-based sources. Eighty percent of debris in the oceans can be attributed to land-based sources (Andrady, 2011), resulting from things like urban litter, mismanaged solid waste (Jambeck et al., 2015), and extreme weather events like flooding (Barnes et al., 2009). In 2010, Jambeck et al. estimates that 83% of the total mismanaged solid waste with the possibility of entering the oceans came from twenty "top-polluter" countries around the world, with an estimated actual range of 4.8 to 12.7 million metric tons entering the ocean. A large portion of land-origin debris reaches the sea by means of transport along rivers, with recent findings implicating ten rivers in Asia and Africa as major polluters (Schmidt et al., 2017). Ocean-based sources of debris like abandoned or lost commercial fishing gear, waste dumped at sea, and goods lost in transport contribute around 20% of the influx of plastic debris (Andrady, 2011).

While most recent research has focused on land-based sources of plastic debris, further investigation in to ocean-origin debris will provide a more accurate description of this type of litter in the coming decades.

Of emerging concern to the marine science community, a significant fraction of marine plastic debris is comprised of particulates of less than 5 mm in size, commonly referred to as "microplastics" (NOAA, A Guide to Plastics in the Ocean). Detection of microplastics in the ocean has been occurring since at least the 1970s, when they began appearing in plankton nets (Van Sebille et al., 2015). Their presence in the ocean can be attributed to a few sources: the breakdown of larger macroplastic debris, microbeads from soaps and personal care products, and microfibers from synthetic clothing or fishing materials (NOAA; Andrady, 2011). Wastewater treatment effluent, while effectively filtered for most macro-plastics, is responsible for transporting a significant amount of microplastic waste from land (Murphy et al., 2016). The fragmentation process and timescale for formation of microplastics from larger debris remains under investigation, though it is estimated to occur in as little as a few weeks once plastic has been introduced to seawater.

The Effects of Marine Plastic Debris

The impacts of plastic debris on the marine environment range from the physiological to the ecosystem level, and include ingestion (Wilcox et al., 2015), entanglement (NOAA Marine Debris Program, 2014), and contaminant transfer (Rochman et al., 2013).

Animal entanglement is one of the most highly visible effects of ocean plastics, with a long history of documented cases involving sea lions, whales, dolphins, sea turtles and seabirds (NOAA Marine Debris Program, 2014). Entanglement threatens the motility of marine wildlife, and jeopardizes their ability to efficiently feed, interact with one another for mating and escape predation (NOAA Marine Debris Program, 2014). Abandoned or lost fishing gear such as nets, ropes, and fishing line is often implicated in cases of entanglement (Raum-Suyuran, 2009), and as such is the focus of efforts to reduce the disposal of fishing gear at sea (NOAA Marine Debris Program, 2015).

Plastic ingestion has been documented in over 40% of marine mammals and 44% of seabirds, along with 62 species of fish and 6 of marine reptiles (Marine Debris, 2016). A study on plastic ingestion in Northern Fulmars found that "92.5% of birds had ingested an average of 36.8 pieces, or 0.385 g of plastics" (Avery-Gomm et al., 2012). Ingested plastics can block the digestive track, resulting in reduced feeding efficacy and starvation (Derraik, 2002, Azarello and Van-Vleet, 1987). The size of plastic debris will limit what is feeding on it; for example 74% of plastic ingested by pelagic fish species in the North and Baltic Seas were found to be of microplastic size (<5 mm) (Rummer et al., 2016). Additionally, chemical odors from bio-fouled plastics have been shown to induce foraging behaviors in at least one species of fish (Savoca et al., 2017).

Of emerging concern is the potential for contaminant transfer from plastic debris, from the leaching of plastic additives such as flame retardants and phthalates, to the absorption of organic contaminants from the surrounding environment and to marine organisms (Engler, 2012; Tanaka et al., 2013; Teuten et al., 2009). Plastic particulates have been demonstrated to absorb a variety of contaminants (Rochmann et al., 2013), and the possibility of transfer to organisms, via ingestion and trophic transfer, is a topic of on-going investigation. As plastics are increasingly identified in the tissues of marine species meant for human consumption, concern has begun to mount surrounding the possibility of contaminant transfer to humans.

Marine plastic debris also presents a range of other problems from the human perspective. Aesthetically, as beaches around the world are clogged with plastic, it detracts from the enjoyment of coastal areas for locals and tourists alike. This has led to a rise in the global awareness about the magnitude of plastic garbage in the ocean, and efforts to mitigate the use of plastics, in particular single-use plastic packaging, are underway in many countries around the world. Unfortunately, as clean-up efforts are being implemented, the financial burden of our plastic problem is becoming increasingly apparent. While ocean currents can distribute waste around the globe at no additional cost, retrieving that volume of waste requires vast monetary and energetic costs.

The Degradation of Plastics

Our problems with plastic waste are inherent to its design: plastic is made to endure. Its benefits- strength, durability, waterproofness, are also its downfall. As earlier described, the bonds that make up the polymer backbone are incredibly strong when compared to peptide bonds in other organic materials. Where plant and animal-based materials will degrade in a matter of days to years and re-enter the carbon cycle, plastics persist.

The processes that contribute to the eventual degradation can be separated in to biotic and abiotic factors, and described by their causative agent:

1. **Photodegradation** – breakdown initiated by ultraviolet radiation from sunlight.
2. **Thermal degradation** – heat-induced breakdown.
3. **Thermo-oxidative degradation** – breakdown in the presence of oxygen.
4. **Hydrolysis** – breakdown in water.
1. **Biodegradation** – breakdown by living organisms.

Figure 3. Graphic adapted from Deep Blue Diving, comparing the length of time for degradation to occur in the ocean for some common marine debris.

Light-induced chemical transformation, particularly by UV-B radiation, is typically the initiating factor of polymer degradation in the environment, at which point other degradation pathways can proceed (Andrady, 2011). De-polymerization by thermo-oxidation proceeds in the presence of oxygen atoms, and reduces the molecular weight of the polymer over time, changing the physical properties and making it susceptible to fragmentation. As bonds are broken, side chains become bioavailable, and biodegradation can proceed. The entire process is mediated by the environmental conditions of the system, including light, oxygen levels, and temperature. At sea, these processes are severely inhibited by the lack of oxygen in the environment and lower

temperatures (Andrady, 2011). Both on land and at sea, the process of polymer degradation is incredibly slow compared to most organic materials (NOAA Marine Debris Program, 2014).

The role that microbial biofilms play in the degradation process of plastics is under recent investigation. Referred to as bio-fouling, the colonization and growth of organisms on the surface of plastic debris in the marine environment can be considered a means of transport for plastics in the ocean. As biofilm forms on floating plastics in the marine environment, it has been demonstrated that they lose their buoyancy and eventually sink below the surface over time (Kaiser et al, 2017). This may partially explain the conclusion of a 2014 study (Cózar et al, 2014) that there is less plastic floating in the open ocean than was expected. Though effectively removing plastics from the ocean surface, sinking due to bio-fouling presents a problem when estimating the current plastic load in the ocean, and when considering clean-up efforts.

Several studies have indicated that microbial communities living on marine plastic debris differ significantly from communities in the surrounding seawater, and that they may also differ from biofilms formed on other material surfaces in the marine environment (Oberbeckmann et al, 2016; Zettler et al, 2013; Debroas et al, 2017; Dussud et al, 2017). Because biofilm formation on any surface is a well-established process in the marine environment, the amount and diversity of data on plastic-associated microbial communities will prove useful in revealing specific patterns of colonization and composition. Microbes belonging to broad groups of complex carbon-degrading bacteria have been identified as abundant members of many plastic-associated communities (Oberbeckmann et al, 2016, Dussud et al, 2018), and several of these families of bacteria have been associated with the biological breakdown of hydrocarbons (Chronopoulou et al, 2014). The fact that plastic is derived from oil and petroleum products has prompted investigation in to the metabolic function of these plastic-associated microbes to determine if they have the genomic potential to be involved in the biodegradation of plastics.

Already in the terrestrial landscape, plastic-specific microbial colonization has been established, and even gone so far as to reveal microbial selection for plastic as a food source. The 2016 isolation of a bacterium (*Ideonella sakaiensis*) that degrades intact polyethylene terephthalate by enzymatic digestion, and then utilizes the resulting carbon as an energy source, is an exciting discovery (Yoshida et al., 2016). Thought to represent a novel evolutionary pathway for energy acquisition, the *Ideonella sakaiensis* enzyme called PETase has spurred several efforts to

investigate its mechanism and attempts to increase its rate of activity (Yoshida et. al, 2016; Han et al., 2017; Austin et al., 2018). Previously identified polymer-degrading microbes include *Rhodococcus ruber C208 (*Orr et al., 2004), *Brevibacillus borstelensis (*Hadad et al., 2005*),* and several thermophilic actinomycetes (Wei et al., 2014), all of which were found to degrade polymer films *in vitro*.

As these organisms have mainly been isolated by culture-based studies, continued investigation of polymer-associated microbial communities using a Next-Generation Sequencing (NGS) approach is necessary to provide a more complete view. Culture-based methods have been widely employed in screening for polymer-degrading bacteria, but are limited by the degree to which microorganisms can be grown *in vitro*, typically thought to represent only a small number of species. An NGS approach allows for broad categorization of the complete microbiome, and will enable future efforts to probe the metabolic potential of the marine plastic microbiome to a greater degree.

The Current Study

This research project aimed to investigate microbial colonization of polymer surfaces in the Arctic marine environment around Tromsø, Norway for the purpose of characterizing and comparing community structure. The overall goals and hypotheses were as follows:

- **Goal #1:** *Improve upon a method to effectively remove and isolate DNA from microbial biofilm on microplastics*.

- **Goal #2:** *Investigate abundance, diversity and notable members of polymer-associated and free-floating marine microbiome (alpha-diversity) by taxonomic identification using NGS*.
    - **Hypothesis I:** Polymer-associated biofilms will include organisms unique from those found in free-floating communities.

- **Goal #3:** *Investigate variation in community structure between polymer-associated biofiolm members and free-living organisms (beta-diversity)*.

- **Hypothesis II:** Variation in community structure will exist between samples of polymer-associated and free-floating organisms.

- **Goal #4:** *Investigate substrate specificity of polymer-associated organisms by measuring diversity between microbial community composition on one polymer compared to another (beta-diversity).*
    - **Hypothesis III:** Variation in community structure will exist between samples of biofilm on one type of polymer versus another.

- **Goal #5:** *Measure surface degradation of submerged polymers by Scanning Electron Microscopy; determine any relationship between microbial community diversity and polymer degradation.*
    - **Hypothesis IV:** If measurable variation in surface degradation state exists between different polymer-types after incubation at sea, that variation may be explained by variation in the community structure of surface biofilms.

Materials and Methods

Experimental Design and Sampling

An immersion experiment as designed to assess variation in microbiome community composition on four different types of pre-production plastic pellets (Low-density polyethylene (LDPE), polypropylene (PP), polystyrene (PS) and polyethylene-terephthalate (PET)) in the Arctic marine environment around Tromsø, Norway. Rubber, a non-synthetic polymer, was used as a control sample.

For each substrate (LDPE, PP, PS, PET, rubber), 5g in pellet form represented one sample. Three replicate samples for each synthetic polymer were immersed at both Location # 1 and Location #2 during the summer sampling season, and two replicates of each were used in the winter sampling. One sample of rubber was used at Location #1 and Location #2 in summer, and none in winter.

Samples were identified throughout the experiment by their substrate type, location (1 or 2), and their sub-sample number (1-3). Any additional identifiers used throughout the study were made based on variations in protocol. **Table 1** below illustrates the number of samples substrate type, location and season (W=winter; S=summer). Color-coding is consistent throughout the material for identifying samples by substrate type.

Substrate	Location 1 (W/S)	Location 2 (S)
PET	n=5/n=3	n=3
PE	n=2/n=3	n=3
PS	n=2/n=3	n=3
PP	n=2/n=3	n=3
H2O	n=2/n=3	n=3
R	n=0/n=1	n=1

Table 1. Number and type of samples submerged at each location in winter (W) and summer (S).

The following sampling set-up was adapted from the protocol used for the JPI Oceans PLASTOX project at NILU in Tromsø.

Each sample (1 sample = 5g pellets) was portioned (**Figure 4** (a)-(c)) in to a reusable teabag and sewn shut. The teabags were grouped by substrate type and encased in nylon mesh sleeves for additional security. Each substrate type was color-coded for identification, then affixed to the inside of a cylindrical metal cage, securing the samples in place while allowing water to pass freely through and around the samples. Cages were affixed to a stationary structure (a dock and boat ramp) and submerged.

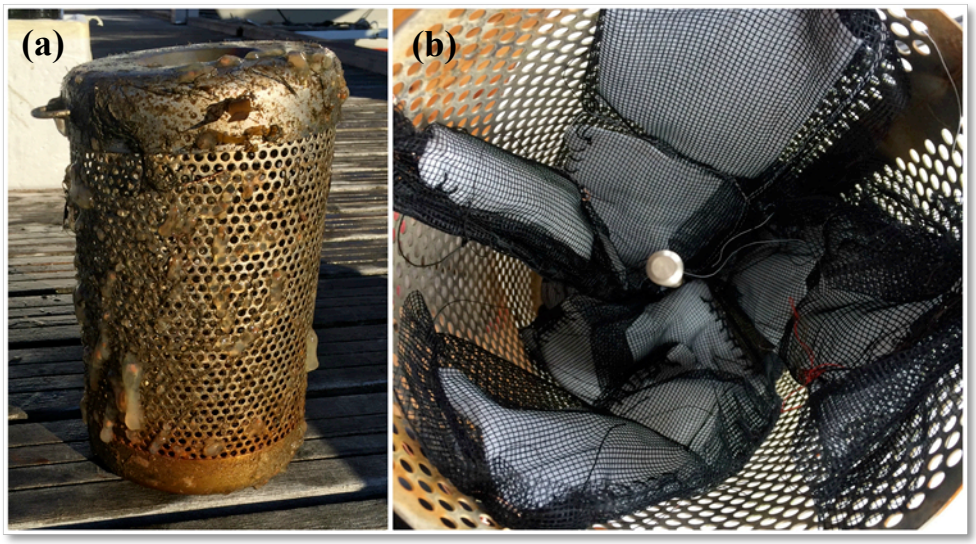

Figure 4. (a) Example cage used for submersion. (b) An inside view of the cage with the nylon sleeves and teabags containing pelletized polymers visible. (c) 2 g samples of microplastic pellets with paper clip for scale.

Sampling locations (**Figure 5**) were chosen to reflect two different micro-environments. Location #1, on the eastern side of the Tromsø island, is heavily trafficked by motorized boats, and is located directly adjacent to the urban center of the island. Location #2, on the western side of the island, is in a less developed area, sees less motorized traffic, and is shallower. At Location #2, the sample cage was subject to periodic tidal shifts that left the samples exposed to the air for parts of the day.

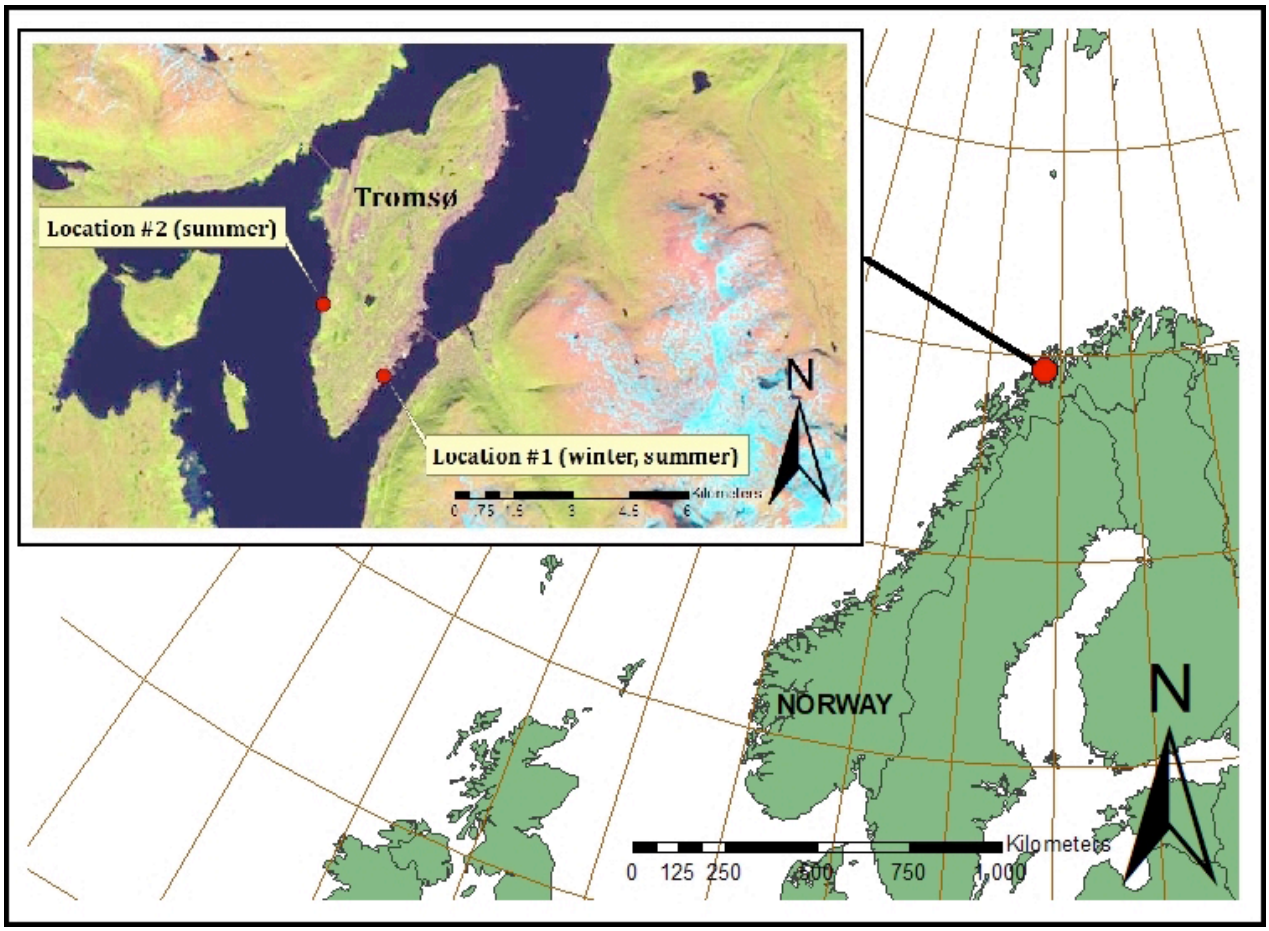

Figure 5. Map of the sampling area. Overview of the geographic area, with sampling Location #1 and Location #2 indicated by the red dots on the in-set map of Tromsø, Norway (Lat: 69.56544°N, Long: 19.41143°E). Map data sources: USGS, Earth Explorer Landsat 8, 2017, August 9; ESRI/ArcGIS Country Boundary Layer.

The first cage was attached to a rope in the small boat harbor near Framsenteret in Tromsø (Location #1), and submerged in the water on November 9, 2016. A temperature and light logger was put in place and began recording on December 2, 2016 at intervals of 15 minutes for the duration of the experiment. This cage and sample set served as a trial set to determine optimal post-immersion processing techniques. Cage #1 remained in the water for 4 months, until March 9, 2017. These samples are referred to in the data as winter season samples.

Cage #2 was submerged at Location #1 near Framsenteret on March 29, 2017 and remained in the water until September 29, 2017. Samples from this cohort are categorized in the data as summer season samples.

Cage #3 was submerged at Location #2, on the west side of the Tromsø island near the University of Tromsø kayak boathouse on April 1, 2017 and was removed from the water on October 4, 2017. These samples are also referred to as summer season samples. At this location, samples were exposed to periodic tidal changes and were alternately submerged and exposed throughout the course of most days.

Seawater Sterilization

Sterilized seawater was used to rinse samples post-immersion to remove any non-attached microorganisms. Water sterilization was achieved using a combination of heat, UV radiation and filtration. This protocol has been developed and verified for sterilization by the University of Tromsø aquaculture lab, and samples of the sterilized seawater were used in the extraction procedures as negative controls to verify the procedure.

Using the system in place at the UiT aquaculture lab, seawater was pumped from the harbor in Tromsø and passed through a 0.22 μm pore filter. Water was then irradiated by UV light before being collected in sterile glassware. The containers were then submerged in boiling water for ten minutes. After sterilization, water was allowed to return to room temperature before being sealed and stored at 4°C for no longer than two weeks prior to extraction.

Biofilm Removal and DNA Extraction

The following protocol was adapted from (Oberbeckmann et al., 2016) and (Wright et al., 2009) for use in removing attached biofilm and extracting DNA.

Several trials of different biofilm removal and subsequent DNA extraction methods were assessed to determine the optimal method for obtaining a high yield of microbial DNA for downstream sequencing.

a. *Trial #1 (the most effective protocol from winter season):*

Winter season samples were submerged at Location #1 and removed at 3 months post-immersion in March 2017. Samples were removed from the water and stored for transport in a sterilized cooler filled with sterilized seawater. At the lab, sub-samples of 10 plastic pellets per sample were transferred to sterile 2 ml Eppendorf tubes and stored at -20°C for 1-2 weeks.

Prior to extraction, 1 ml of UltraPure RNA-free water was added, and samples were incubated on a heating block at 15°C for 15 minutes. Samples were then ribolyzed twice for 30 seconds each. The plastic pellets were removed from the sample tube and the presumed biofilm pellet was resuspended in UltraPure water. Following the rinse process, DNA extraction was performed on approximately 700 μl of starting material using the UltraClean Microbial DNA Isolation kit from MoBio (Qiagen, Hilden, Germany) following the manufacturer's protocol. Samples were stored at -80°C for several months post-extraction.

b. Trial #2:

For summer season samples submerged in the Tromsø harbor and at the kayak house, removed at 6 months post-immersion in October 2017, the rinsing and DNA extraction procedures were extensively modified in an effort to produce higher extraction yields.

All equipment used was sterilized in an autoclave or washed then triple-rinsed with 70% ethanol followed by DI H_2O. Seawater used for rinsing was sterilized following the previously detailed protocol.

At water's edge, sample cages were removed and sample types sorted according to their labels. Sample packets were rinsed with sterile seawater, cut open, and the contents transferred to 15 ml

Falcon tubes for transport to the lab in a cooler. Samples were stored at -20°C for approximately 1 week before extraction.

Prior to extraction, 0.5 g sub-samples (approximately 10-12 pellets per sample) were taken from storage, suspended in 700 μl of lysis buffer (40 mM EDTA, 50 mM Tris in MQ H20, adjusted pH 7.2) and incubated at 15°C for 1 hour with shaking to loosen biofilm. Samples were incubated and shaken with 100 μl lysozyme (125 mg/ml final in TE buffer: 10 mM Tris, 1 mM EDTA, pH adj = 8.2) at 37°C for 1 hour, then 20 μl RNase A (10 μg/ml) at 37°C for 30 minutes. Next, samples were incubated in 100 μl Proteinase K (Qiagen) and 100 μl 20% SDS buffer (20% w/v SDS in TE buffer) for 1 hour at 55°C. Samples were centrifuged at 8,000 g for 10 minutes, plastic pellets were removed, and the resulting lysate solution was re-suspended and transferred to a new 2 ml Eppendorf tube.

Equal volume (approximately 1 ml) Phenol:Chloroform:Iso-amyl alcohol (25:24:1, Sigma-Aldrich, St. Louis, MO, USA) was added to the lysate solution and vortexed for 10 seconds. Tubes were centrifuged at 2,500 g for 5 minutes and the resulting aqueous layer was transferred to a new 2 ml tube, leaving behind a thin aqueous layer to avoid contamination. Equal volume (approximately 1 ml) Chloroform:Iso-amyl alcohol (24:1, Sigma-Aldrich) was added, samples were vortexed for 10 seconds, then centrifuged at 2,500 g for 5 minutes. The aqueous layer was transferred to a new Eppendorf tube, 1 ml of TE buffer (10 mM Tris, 1 mM EDTA, pH adj = 8.2) was added, and samples were vortexed.

The entire solution was transferred to the filter compartment of an Amicon Ultra-4 centrifugal filter unit (MilliporeSigma, Burlington, MA, USA) to clean and concentrate the DNA extract. Tubes were centrifuged at 3,500 g for 5-10 minutes, or until less than 1 ml of solution remained in the filter compartment. The flow-through was removed and stored in another Falcon tube until DNA concentration in the retentate could be verified. Two ml of TE buffer was added to the filter compartment and samples were spun again at 3,500 g for 5-10 minutes, or until less than 1 ml of solution remained in the filter compartment, the flow-through was removed and stored. This was repeated twice for a total of 3 rinses. 50 μl of the final retentate was transferred to a 2 ml Eppendorf tube and stored at 4°C to serve as the working stock, and the remaining retentate (approximately 200-500 μl) was stored at -20°C for approximately 1 week until submission to LGC Genomics Laboratory for sequencing.

DNA concentrations in the retentate and flow through were measured on a NanoDrop 2000c Spectrophotometer (ThermoFisher Scientific, Waltham, MA, USA) to verify successful extraction and concentration prior to proceeding with amplification and sequencing.

Seawater Sample Collection and Filtration

The following protocol was adapted from Walsh et al. 2009.

Seawater samples were taken to determine the community composition of the free-floating microbiome in seawater for comparison to the polymer-attached microbiome. Three 1 liter samples of seawater were taken at Locations # 1 and #2 at the same time as the summer season samples were removed from the water in autumn 2017.

Seawater sample collection was carried out using one liter glass containers, sterilized prior to use with triple rinses of 70% ethanol followed by DI H_2O. Sample containers were immersed in the sea to a depth of approximately 1 meter, opened, filled and capped before being brought back to the surface. Containers were transported to the lab immediately following collection and stored at 4°C for one day prior to filtration.

Samples were mixed prior to processing to account for settling that may have occurred overnight. They were then measured using a graduated cylinder to ensure a uniform volume for filtration. Each one liter sample was hand filtered using a new sterile 50 ml syringe, attached at one end to a sterile 0.22 μm pore size Sterivex filter (Sigma-Aldrich) Once the entire volume was passed through the Sterivex filter, the syringe was used to evacuate any residual water from the filter compartment, 1.8 ml lysis buffer (40 mM EDTA, 50 mM Tris in MQ H20, adjusted pH 7.2) was added and both ends were sealed with parafilm before storage in a 50 ml Falcon tube at -20°C.

Prior to extraction, the filters were removed from the freezer and allowed to thaw. They were then subject to the same extraction protocol as detailed above for Trial #2 of biofilm extraction, including enzyme incubations, phenol-chloroform extraction, and concentration in Amicon Ultra tubes, with solvent volumes adjusted to account for the additional starting volume.

Target Sequence Amplification and Illumina MiSeq Library Generation

Twenty-five samples of DNA extract were submitted to LGC Genomics (Berlin, Germany) for 16S, 18S and ITS2 rRNA gene amplicon sequencing for bacterial, eukaryotic and fungal taxonomic identification using the Illumina platform. **Table 2** contains information on the number and type of samples selected for sequencing. Selection was based on quantity and quality of DNA as measured on the Nanodrop spectrophotometer (DNA concentration > 20 ng/ μl, 260/280 nm ratio = 1.8-2.0, at least 60 μl extract volume).

Substrate	Location 1	Location 2
PET	n=3*	n=3
PE	n=2	n=2
PS	n=2	n=3
PP	n=2	n=3
H2O	n=2	n=2
R	n=1	n=0

Table 2. Depicts the number and substrate of each biofilm sample submitted to LGC Genomics for sequencing. Rubber was not available for inclusion at Location #2. *One PET biofilm sample from the winter trial at Location #1 was adequate for sequencing, along with two samples from the summer season. The rest of all biofilm extracts came from summer samples.

The following graphic (**Figure 6)** shows the 16S rRNA gene that was targeted for amplification of bacterial isolates. Primers pairs target the constant regions; these regions are highly conserved across all bacterial taxa, while the variable regions in between are used for uniquely identifying them by their sequence. The same approach was used for both 18S and ITS gene amplification.

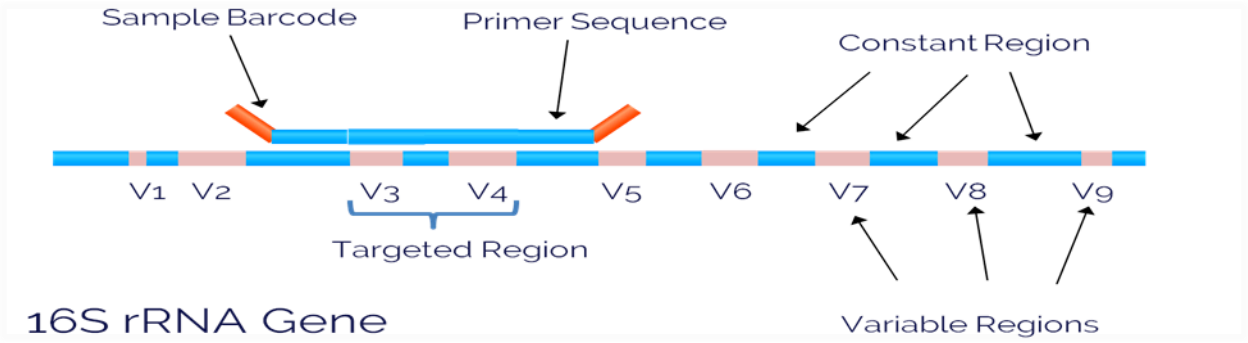

Figure 6. Structure of 16S rRNA gene, the target of PCR to identify bacterial communities in biofilm extracts. The figure shows approximately where primers bind to the amplicon, and indicates the targeted variable regions used for taxonomic identification. Adapted from https://www.visionscape-sanitation.com/tackling-ocean-plastic-pollution-with-key-infrastructure/.

Primer pairs used to target genes for amplification were as follows:

- **16S:** *341F (5' -CCTACGGGNGGCWGCAG-3') and 785R (5'-GACTACHVGGGTATCTAAKCC-3')*
- **18S:** *Eu565F (5'-CCAGCASCYGCGGTAATTCC-3') and Eu981R (5'-ACTTTCGTTCTTGATYRATGA-3')*
- **ITS:** *ITS7F (5'-GTGARTCATCGAATCTTTG-3') and ITS4R (5'-TCCTCCGCTTATTGATATGC-3')*

Primer pair design was chosen based on recommendations from LGC Genomics and the following references for 16S, 18S and ITS amplification, respectively: (Ihrmark et al., 2012; Klindworth et al., 2012; Stoeck et al., 2012). These primers were chosen to ensure inclusivity of the greatest number of taxa for accurate representation of the complete microbiome. The 18S primer pair Eu565F and Eu981R is an in-house design by LGC Genomics Laboratory; it is a

slightly modified version of the Stoeck primer pair made by adding 3 bases at the 3 prime end to improve PCR outcome.

Inline barcodes were generated for each sample to uniquely identify them post-multiplexing, and were added to the 5' end of the forward and reverse primers, and are included in Appendix 1, **Table A**.

PCR reactions were carried out in 96 well plates. Each well was prepared with 20 μl of MyTaq buffer (Bioline, London, UK) containing 1.5 μl MyTaq DNA polymerase, and 2 μl BioStabll PCR Enhancer (Sigma-Aldrich). Sample extract was added at volumes corresponding to approximately 5 ng template DNA, with exact volumes differing for each sample based on the extract's DNA concentration. Forward and reverse primers were added to each reaction well at concentrations of 15 pmol/vol.

PCR reactions were carried out using the following thermal cycle specifications:

- 1 min 96°C **(Initialization)**
- 96°C for 15 seconds **(Denaturation)**
- 50°C for 30 seconds **(Annealing)**
- 70°C for 90 seconds **(Elongation)**

16S and ITS2 amplicon plates were run for a total of 30 cycles, and the 18S amplicon plate was run for a total of 38 cycles.

Post-PCR, samples were run on a 1% agarose gel at 120 V for verification of successful amplification prior to sequencing.

Amplified samples were sequenced by paired-end reading of approximately 300 base pairs at a depth of 5 million read pairs on an Illumina MiSeq Personal Sequencer using MiSeq Reagent Kit V3 (Illumina, San Diego, CA, USA).

Sequence Data Processing

a. Data pre-processing for all amplicons

De-multiplexing of the library groups was performed using the Illumina bcl2fastq 2.17.1.14 software, and samples were sorted according to the amplicon of interest. At this stage, one or two mismatches or Ns were allowed in the barcode read when distances between all libraries on the lane allowed for it. Further de-multiplexing sorted samples according to their inline barcodes and verification of restriction site. No mismatches or Ns were allowed in the inline barcodes, but Ns were allowed in the restriction site. Sequencing adapter remnants were clipped from all reads, and those with a final length of <100 base pairs were discarded. Primers were assessed according to the following specifications: primer pairs present in the sequence required, 3 mismatches allowed per primer, if primer-dimers detected outer primer copies clipped. Sequences were oriented into forward-reverse primer direction after removal of the primer sequences. Forward and reverse reads were combined in to consensus sequences using BBMerge 34.48.

b. 16S prokaryotic community analysis data processing

16S amplicon samples were processed and operational taxonomic units (OTUs) picked using Mothur 1.35.1. Sequences containing ambiguous bases, homo-polymer stretches of more than 8 bases, and those with an average Phred quality score below 33 were removed. Samples were aligned against the 16S Mothur-Silva SEED r119 reference alignment. Truncated or unspecific PCR products were filtered out. Error reduction was implemented by pre-clustering and allowing for up to one differing base per 100 bases in a cluster. Chimeras were eliminated using the unchime algorithm. Sequences were organized by taxonomical classification using the Silva reference classification, and sequences from other domains ("Eukaryota-Chloroplast-Mitochondria-unknown") were removed. OTUs were picked by clustering at the 97% identity level using the cluster.split method. Consensus for taxonomical calling was reached by integrating the taxonomical classification of cluster member sequences. A phylogenetic tree was generated using the FastTree method.

Species level annotation of OTUs was carried out using NCBI BLAST+ 2.2.29. Representative sequences with at least two observations were queried against known and classified sequences in

the ribosomal database project (release 11.4). BLAST+ parameters were set at E<= 0.1 and percent identity >= 90%. A summary table was generated with taxonomy and alignment details for the 20 best hits for each OTU representative sequence.

OTU diversity was analyzed using QIIME 1.9.0. OTU abundance patterns were exported in Cytoscape format as an OTU network and analyzed for alpha and beta-diversity, with samples grouped based on sample and location type.

c. 18S eukaryotic community analysis data processing

Data processing for 18S amplicon sequences followed the same protocol as processing for the 16S amplicons, the only exceptions being alignment against the 18S Mothur-Silva SEED r119 reference alignment, and the exclusion of species level annotation of OTUs using BLAST+.

d. ITS fungal community analysis data processing

Data processing for ITS amplicon samples also followed a similar protocol, with sequence processing and OTU picking using Mothur 1.35.1. Truncated sequences were filtered out, a sub-sample of 40,000 sequences per sample was taken, chimeras were eliminated, and samples were clustered at the 97% identity level. Cluster representative sequences were altered from the default state of longest sequence to selection of the most abundant sequence. Clusters with less than 100 observed sequences were filtered out. OTUs were taxonomically classified using the UNITE reference database (version 6). OTU diversity analysis using QIIME 1.9.0 proceeded according to the same protocol as used for 16S amplicon data processing.

Diversity Measurement and Statistical Analysis

Taxonomically binned OTU count tables were filtered to exclude OTUs with less than two counts. Bar charts depicting the relative abundance of taxa were generated in QIIME at the most descriptive order for each group, and a taxonomic identification legend was generated for the top ten most abundant taxa over all substrate types.

Samples were grouped by substrate type, and alpha rarefaction curves were generated to compare species richness over a range of sequencing depths for each substrate type. Sequence counts were normalized for all samples by randomly resampling at two different levels: the median rarefaction level, and a level selected to reflect accurate diversity while preserving sample size. Samples were analyzed for alpha diversity at both rarefaction levels by substrate type and location using Species Richness and Chao 1 diversity indexes by pairwise t-tests.

Rarefied data was grouped by substrate type and location and analyzed for beta-diversity using QIIME 1.9.0 at each meta-level. The workflow for beta-diversity analysis is as follows:

1. Weighted Unifrac distance matrices, a method for measuring diversity between microbial communities based on the abundance of OTUs and their phylogeny (Lozupone & Knight, 2005), were generated for each group (bacteria, eukaryotes, fungi).
2. The values in these matrices were used to measure variation between two different types of distances: distances *within* groups (i.e. Group 1: H2O vs. H2O) to distances *between* groups (i.e. Group 2: H2O (a) vs. PET (b)) using pairwise two-sided student's t-tests with 999 Monte Carlo permutations.
3. Principal coordinate analysis (PCoA) plots were generated using Emperor 0.9.60 (EMPeror, 2013). Emperor uses coordinate data based on the phylogenetic distances in weighted Unifrac tables to generate a three-dimensional plot of the distances.

Scanning Electron Microscopy (SEM)

a. Sample preparation

On removal from the water, individual sample pellets were transferred to a 1.5 ml Eppendorf tube for transport to the SEM lab at the Department of Biomedicine at UiT. Samples were transported from the water to the lab within approximately one hour.

Following standard protocol of the SEM lab for fixation of biological samples, the samples were immersed in a 4% glutaraldehyde solution overnight at room temperature. They were then rinsed twice for 15 minutes in phosphate buffer solution, followed by immersion in 1% OsO_4 in ddH_2O for 30 minutes. Samples were again rinsed twice for 15 minutes in phosphate buffer.

Following fixation, samples were dehydrated by immersion in a graded series of ethanol solutions:

1. 60% ethanol for 5 minutes.
2. 90% ethanol for 5 minutes.
3. 96% ethanol for 5 minutes.
4. 100% ethanol 4x for 5 minutes each.

Samples were removed and dried in a critical point drier before being mounted on SEM-studs using carbon tape and silver glue, then coated with gold and palladium in a sputter coater. Samples were stored at room temperature and imaged within 3 weeks.

b. Imaging and processing

Samples were imaged at the University of Tromsø Scanning Electron Microscopy Lab on a Zeiss Sigma SEM with spatial resolution of 1.5 nm at EHT=1 kV. Images of pre-immersion and post-immersion pellets were taken at the same magnification (5.00 K X) at WD=2.5 mm and EHT=2.00 kV.

Image processing was done on ImageJ software to attempt to quantify variation in surface degradation using the roughness measure tool.

Results

Temperature Log

Seawater temperature was recorded at sampling Location #1 at Framsenteret for the duration of the experiment from December 2016 through December 2017. Winter (Dec. – Mar.) and summer (Apr. – Oct.) average temperatures were calculated (W avg. = 4.8°C; S avg. = 7.8°C) to determine the average conditions samples were exposed to during their incubation period. Temperature ranged from a minimum 2.3°C in February 2017 to a maximum of 13.7°C in August 2017.

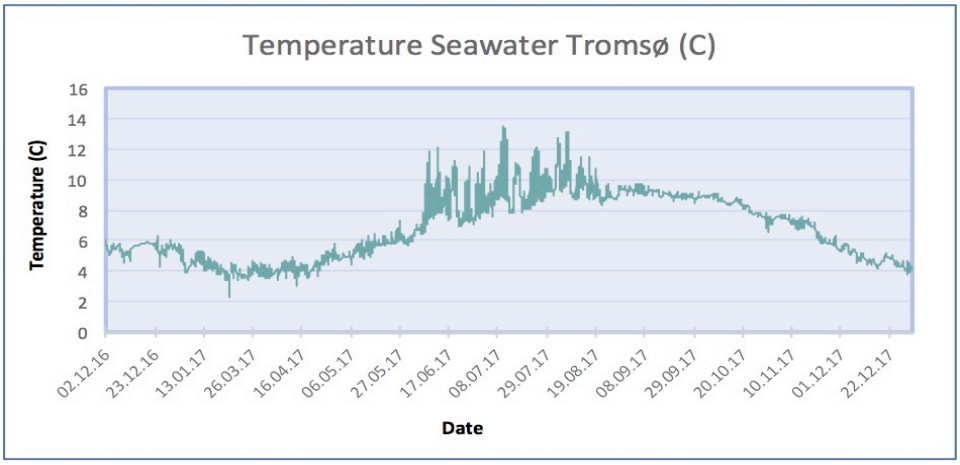

Figure 7. Graph of seawater temperature in Tromsø, taken at sampling Location #1 from December 2016 – December 2017. (Min: 2.3°C; Max: 13.7°C; Winter avg. (Dec. '16-Mar. '17): 4.8°C, Summer avg. (Apr. '17-Oct. '17): 7.8°C, Yearly avg. (Dec. '16-Dec. '17): 6.8°C). *The information used to generate this graph was provided by Dorte Herzke of NILU*.

DNA Concentrations in Extracts

Samples selected for sequencing were limited to those of sufficient quantity and quality ((DNA concentration > 20 ng/ μl, 260/280 nm ratio = 1.8-2.0, at least 60 μl extract volume) after DNA extraction. With the exception of sample PET-DR-10, all winter season samples were below the necessary DNA concentration level and were not suitable for sequencing. Twenty-four samples from the summer season were viable candidates for sequencing.

PCR Amplification of 16S, 18S and ITS Regions

The following gel images (**Figures 8(a)-(c)**), were taken by LGC Genomics after PCR amplification of the 16S, 18S and ITS regions of DNA extracted from samples. Amplification was for the most part successful, with rubber samples being excluded from ITS analysis.

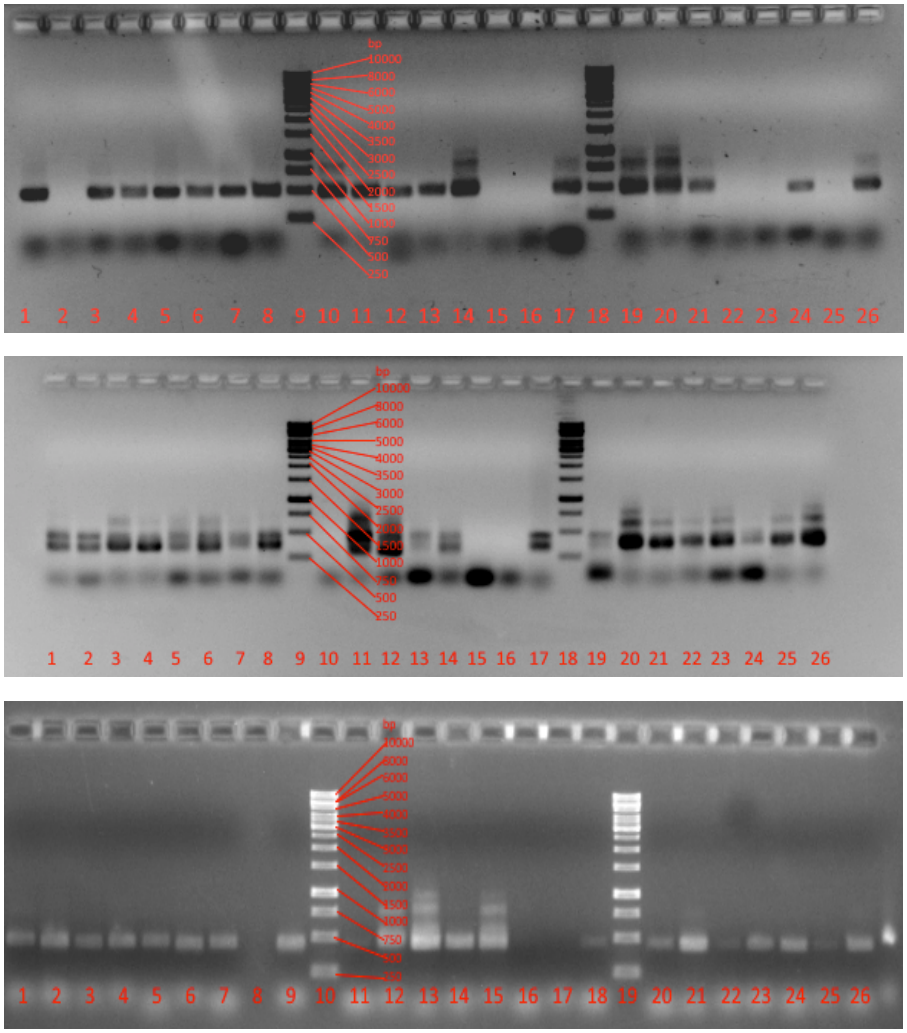

Figure 8. (a). Gel image of 16S amplicon from DNA extract samples after PCR. Sample order by well (1-26): PET 1-3, PET 1-2, PE 1-2, PE 1-1, PS 1-3, PS 1-2, PP 1-2, PP 1-1, 1 kb DNA ladder, R 1-1, H2O 1-1, H2O 1-3, H2O 2-1, H2O 2-3, DR-10, PET 2-1, PET 2-2, 1 kb DNA ladder, PET 2-3, PP 2-1, PP-2-2, PP 2-3, PS 2-1, PS 2-2, PS 2-1, PE 2-2. **(b).** Gel image of 18S amplicon from DNA extract samples after PCR. Sample order unknown. **(c).** Gel image of ITS2 amplicon from DNA extract samples after PCR. Sample order by well (1-26): PET 1-3, PET 1-2, PE 1-2, PE 1-1, PS 1-3, PS 1-2, PP 1-2, PP 1-1, 1 kb DNA ladder, R 1-1, H2O 1-1, H2O 1-3, H2O 2-1, H2O 2-3, DR-10, PET 2-1, PET 2-2, 1 kb DNA ladder, PET 2-3, PP 2-1, PP-2-2, PP 2-3, PS 2-1, PS 2-2, PS 2-1, PE 2-2.

Relative Abundance and Taxonomic Identification

In total, twenty-five 16S-amplified samples resulted in 705,037 sequences of 10,697 OTUs (Table density (fraction of non-zero values): 0.187 counts; Min sequence count: 10; Max: 39,316; Median: 35,568; Mean: 28,201; Std. dev.:13,377). Twenty-four 18S-amplified samples resulted in 714,261 sequences of 5,371 OTUs (Table density: 0.134; Min sequence count: 60; Max: 39,706; Median: 39,121; Mean: 29,761; Std. dev.: 13,678). Twenty-five ITS-amplified samples resulted in 649,755 sequences of 1,372 OTUs (Table density: 0.119; Min sequence count: 5; Max: 39,972; Median: 35,606; Mean: 25,990; Std. dev.: 14,402).

The relative abundance of the top ten most abundant taxa per amplicon is depicted in **Figures 9-11**, with samples grouped by substrate type.

A. Bacteria

In 16S samples, Gammaproteobacteria were the most dominant bacterial taxa in seawater, polypropylene and rubber samples (Seawater: 39.77%, mainly *Colwellia* sp.; Polypropylene: 24.03%; Rubber: 66.82%, mainly 34P16). Alphaproteobacteria were the most dominant taxa present on, polyethylene-terephthalate, polyethylene and polystyrene samples (24.12%, 25.22%, and 24.28%, respectively).

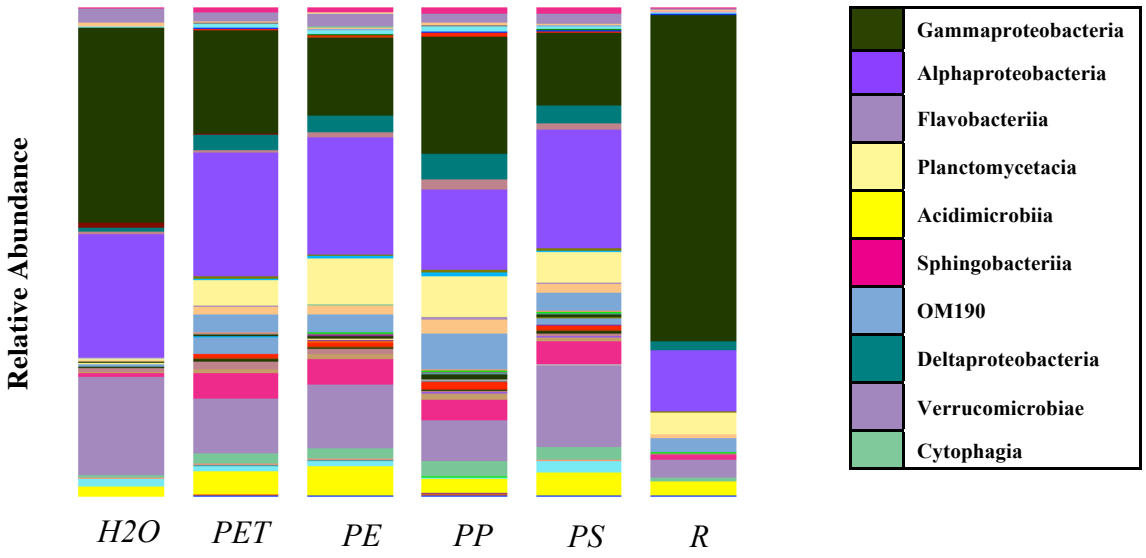

Figure 9. Relative abundance of bacterial OTUs.

B. Eukaryotes

Among Eukaryotic communities, the most common group identified in seawater samples was Holozoa (38.72%, mainly Arthropoda). Holozoa were also prevalent members of all polymer-associated biofilms, ranging from 12.5% prevalence on PE pellets to 24.75% on rubber samples. Chloroplastida were abundant members of PE, PP and PS biofilms (29.47%, 20.19% and 17.89%, respectively). Their presence in PET, rubber and seawater samples was less than 4%. The most abundant members of PET biofilms were Alveolata (40.51%), and Stramenopiles (28.09%). Stramenopiles was the most common member of PP-associated biofilm (31.48%). On rubber samples, 36.08% of OTUs identified were unclassified beyond the domain level.

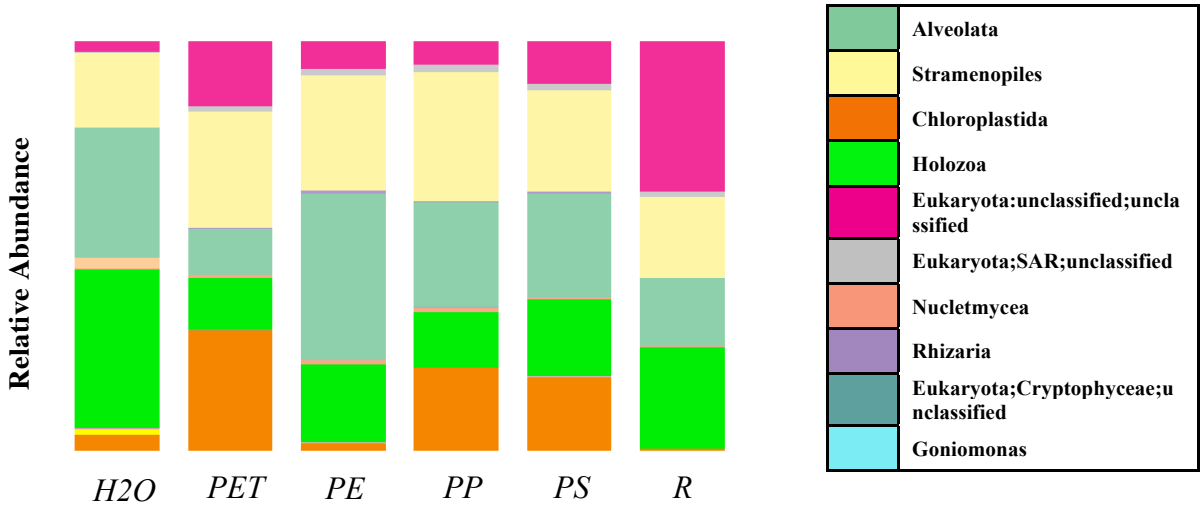

Figure 10. Relative abundance of eukaryotic OTUs.

C. Fungi

Among fungal communities, most OTUs were unidentified beyond the domain level (unidentified OTUs represented in yellow in the chart below). In seawater samples, 52.72% of OTUs were identified as Ascomycota; Ascomycota were also present on polymer samples ranging from 1.12% on PE samples to 11.87% on PET samples.

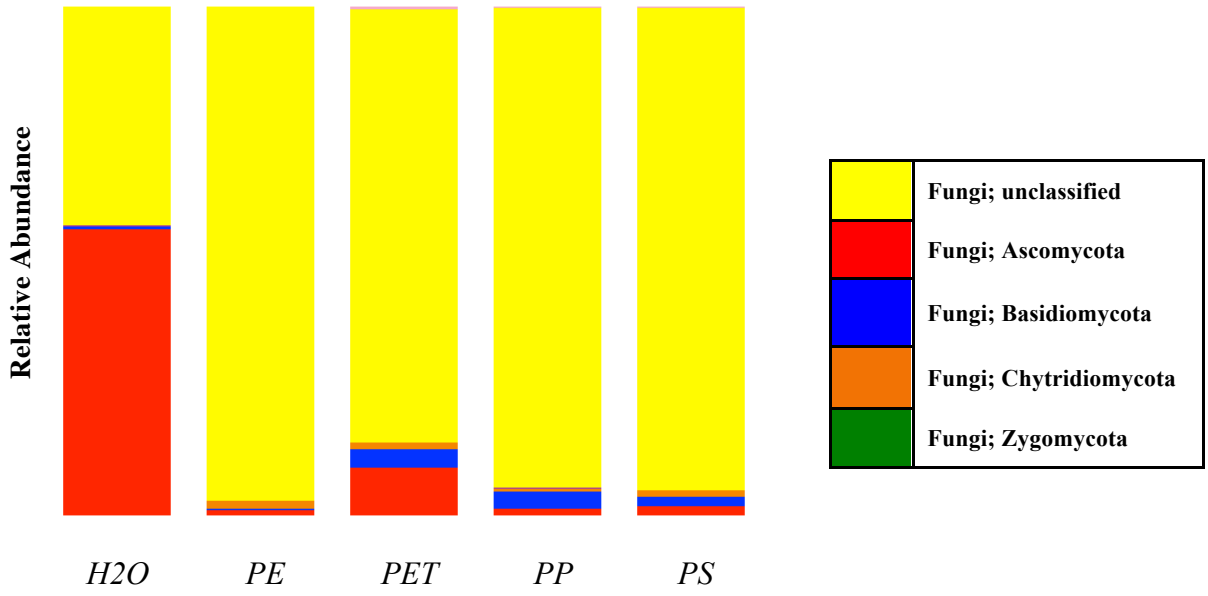

Figure 11. Relative abundance of fungal OTUs.

Alpha-diversity *(within-sample diversity)*

Alpha rarefaction curves depicting the relationship between the number of sequences per sample and the number of species observed were used to determine the optimal rarefaction level for diversity analysis (**Figures 12(a)-(c)**) The results suggest that bacterial, eukaryotic and fungal diversity each approached an asymptote as the number of sequences per sample increased. However, as sequence counts increased, several samples were excluded from the results due to insufficient sequencing depth. To preserve sample size in an already limited sampling pool, diversity analysis was performed on data rarefied to the lower sequence count, corresponding to the point where diversity begins to appear asymptotic (16S: 3,500 sequences/sample; 18S: 4,500 seqs/sample; ITS: 4,100 seqs/sample). In some cases, alpha-diversity comparisons from the

higher rarefaction level are included for comparison. The average number of observed species at the selected rarefaction level for analysis is presented in the boxplot to the left for each substrate.

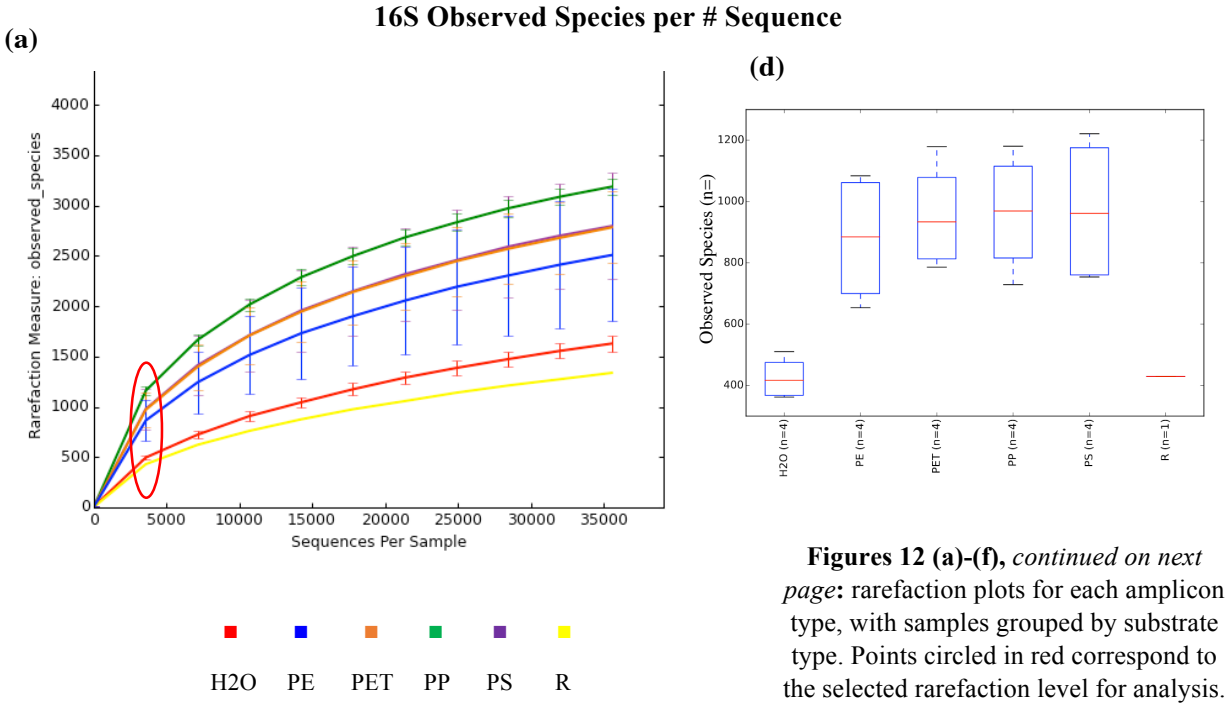

Figures 12 (a)-(f), *continued on next page***:** rarefaction plots for each amplicon type, with samples grouped by substrate type. Points circled in red correspond to the selected rarefaction level for analysis. Lines are color coded by substrate type. Figures d-f in the right column show the average number of species for substrate-grouped samples at the selected rarefaction level.

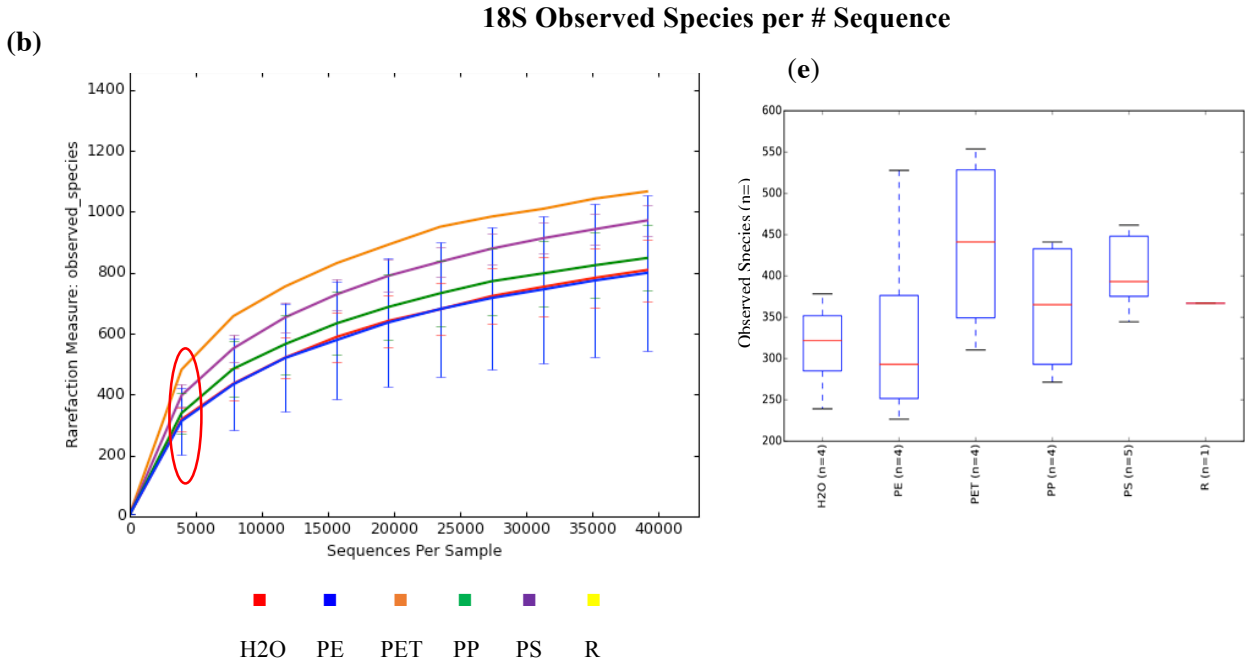

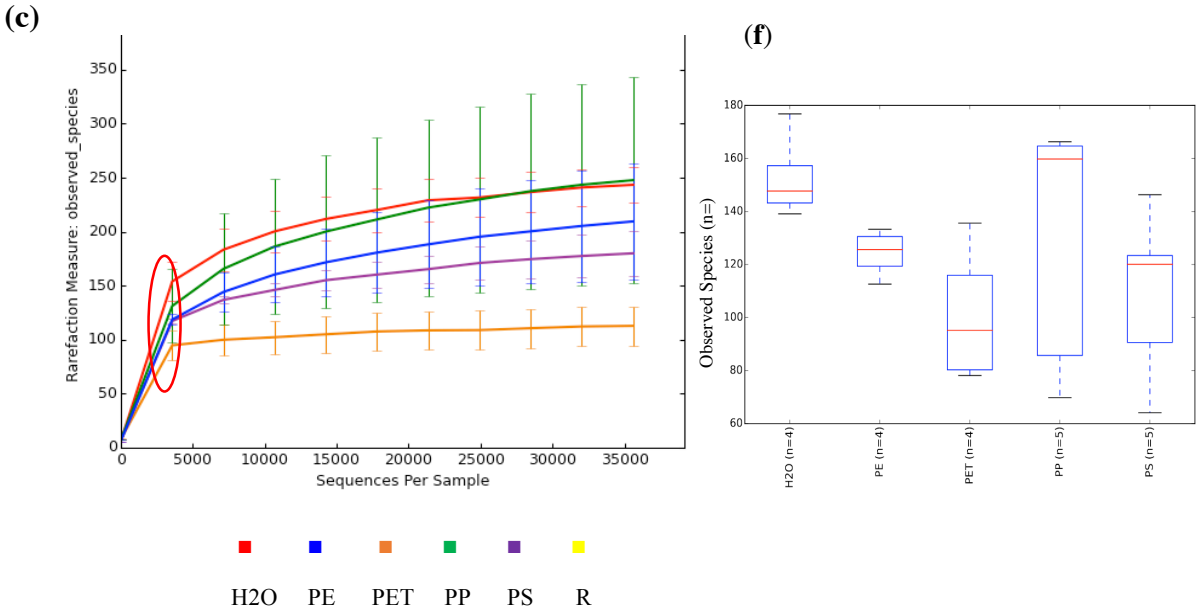

No significant differences in alpha diversity metrics were found in the comparisons of free-living (F) to plastic-associated (A) communities for any substrate types. No significant differences in Observed Species were noted for any groups, but Chao 1 diversity indexes differed significantly between Location 1 and 2 for both 18S and ITS communities (18S p-value: 0.045; ITS p-value: 0.035).

Substrate	PET	PE	PS	PP	All
Subgroups	F · A	F · A	F · A	F · A	1· 2
Bacteria (16S)					
Observed Species	5.309 (0.18)	3.829 (0.075)	4.2 (0.39)	4. 812 (0.39)	1.882 (0.08)
Chao 1	5.223 (0.45)	-3.072 (0.435)	3.301 (0.39)	5.045 (0.45)	2.01 (0.068)
Eukaryotes (18S)					
Observed Species	1.828 (1.0)	-0.268 (1.0)	2.459 (.765)	0.858 (1.0)	1.586 (0.151)
Chao 1	0.741 (1.0)	-0.284 (1.0)	1.64 (1.0)	0.582 (1.0)	1.978 **(0.045)**
Fungi (ITS2)					
Observed Species	-3.261 (0.22)	2.998 (0.11)	-2.472 (0.41)	0.937 (1.0)	-1.508 (0.138)
Chao 1	-3.626 (0.37)	1.248 (1.0)	-2.381 (0.57)	0.286 (1.0)	-2.275 **(0.035)**

Table 3. Alpha-diversity metric comparisons by amplicon, substrate and location.

Beta-diversity *(between sample diversity)*

Presented below are the results of beta-diversity analyses based on weighted Unifrac distance matrices (matrices included in Appendix 1) generated from rarefied OTU count tables.

The following PCoA plots are a visual representation of the weighted Unifrac distance matrices based on bacterial phylogeny (Tables B-D, Appendix 1). Samples that are closer together are more *similar*, and samples that are further apart are more *dissimilar*. Samples are clearly grouped by location in each plot (Location 1 and Location 2, displayed on plot), with some grouping by substrate type (color-coded key) within the same location.

a. Bacteria

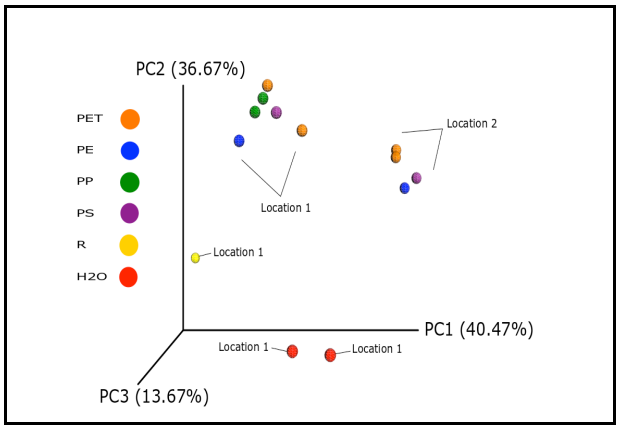

b. Eukaryotes

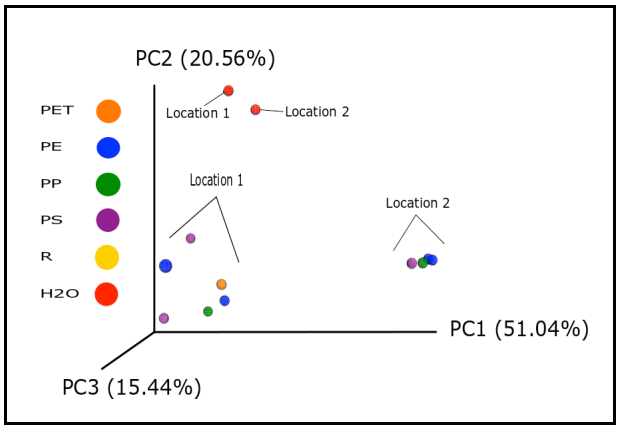

c. Fungi

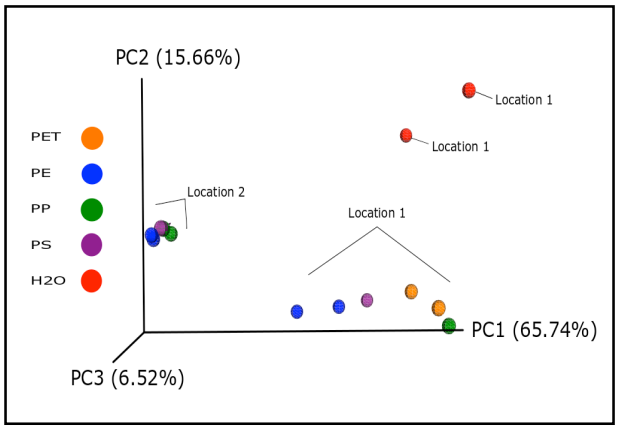

Figure 13 (a) – (c). PCoA plots generated from distance coordinates from corresponding weighted Unifrac matrices.

A. Bacteria

Distances within and between groups are visually depicted in the boxplot below (**Figure 14**) as an example of how distances were compared, and were calculated using the weighted Unifrac matrix for bacterial OTUs included in Appendix 1 Table B. From left, the "All within Substrate" group refers to the average of all distances between samples from the *same* substrate groups, while "All between Substrate" refers to the average of all distances between samples from *different* substrate groups. Distance between different substrate samples was on average greater than distance within same substrate samples, indicating that same-substrate samples were more similar than different substrate samples. Paired groupings represent distances between all samples of the indicated substrates. Variation was measured using these distance totals.

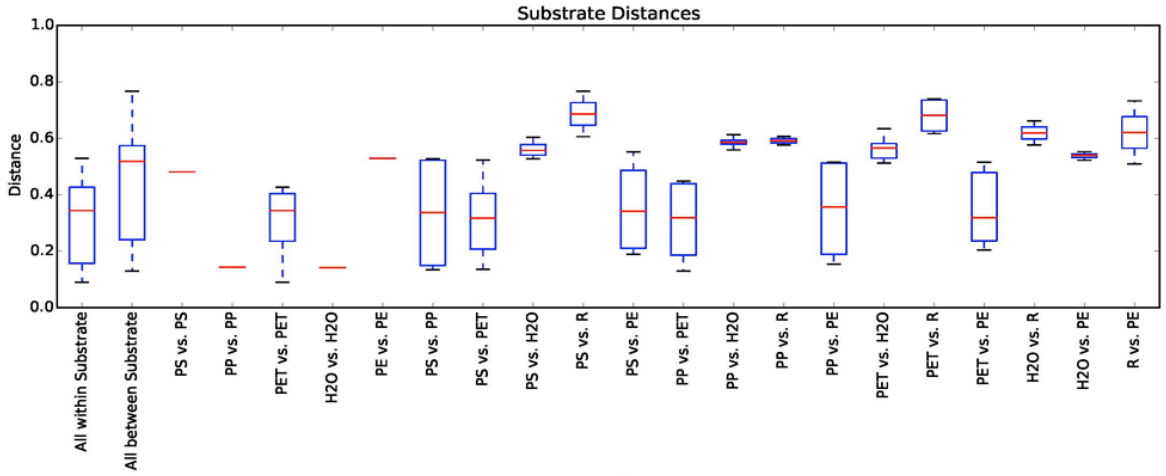

Figure 14. Distance boxplots for 16S amplicon OTUs.

Variation in the composition of bacterial communities was significant (p-values < 0.05) for comparisons between all synthetic polymer-associated biofilm samples and free-floating bacterial communities (H2O samples). Variation between synthetic polymer biofilms and rubber (non-synthetic control) was significant for PS, PP and PET. **Table 4** below indicates all groupings subject to testing. Significant p-values are noted with an (*) on the table.

Group 1	Group 2	T-statistic	Nonparametric p-value
PS	PP	0.619	0.526
PS	PET	0.872	0.39
PS	H2O	-3.351	*0.009
PS	R	-3.460	*0.015
PS	PE	0.296	0.765
PP	PS	0.739	0.464
PP	PET	0.889	0.378
PP	H2O	-3.198	*0.003
PP	R	-2.882	*0.029
PP	PE	0.511	0.596

PET	PS	0.047	0.957
PET	PP	-0.083	0.935
PET	H2O	-5.942	*0.001
PET	R	-5.541	*0.006
PET	PE	-0.513	0.628
PE	PS	0.376	0.699
PE	PP	0.455	0.651
PE	PET	0.484	0.62
PE	H2O	-3.063	*0.007
PE	R	-2.135	0.104

Table 4. Results of two-sided student's t-test with 999 Monte Carlo permutations on Weighted UniFrac distance matrix. Note that Group 1 and Group 2 titles have been simplified to reflect the results; see Materials & Methods section on diversity measurements and statistical analysis (pp 27-28) for explanation of group comparisons.

B. Eukaryotes

Distance boxplots are included here for eukaryotic communities to illustrate the difference in the distribution of ranges compared to the bacterial community distances.Values were calculated using the weighted Unifrac matrix for eukaryotic OTUs included in Appendix 1, **Table C**. Average distances within and between substrates were similar overall. Variation was calculated using paired distances.

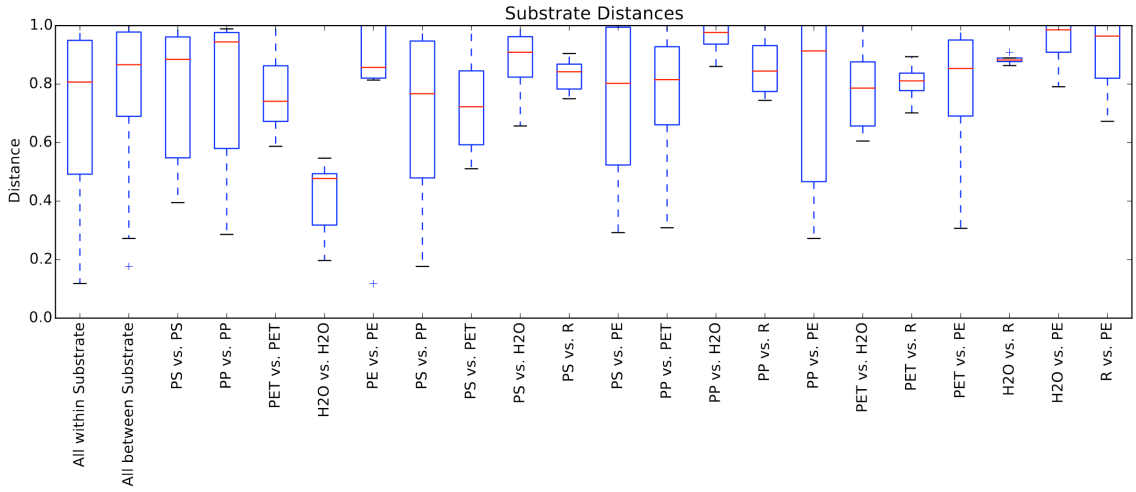

Figure 15. Boxplots of the distances between eukaryotic microbial life on different substrate types. Values based on weighted Unifrac distance matrix, Appendix 1, Table C.

Variation in eukaryotic microbial community structure was significant only between free-living and polypropylene biofilm members (p-value: 0.028) and is denoted with an (*) on the table below. All other comparisons were non-significant.

Group 1	Group 2	T-statistic	Non-parametric p-value
PS	PP	0.604	0.565
PS	PET	0.289	0.769
PS	H2O	-1.563	0.145
PS	R	-0.465	0.634
PS	PE	0.094	0.926
PP	PS	0.415	0.68
PP	PET	-0.065	0.952
PP	H2O	-2.647	*0.028
PP	R	-0.565	0.599
PP	PE	-0.012	0.983
PET	PS	0.244	0.802
PET	PP	-0.028	0.981
PET	H2O	-0.307	0.73
PET	R	-0.360	0.678
PET	PE	-0.587	0.553
PE	PS	0.485	0.622
PE	PP	0.403	0.701
PE	PET	0.054	0.955
PE	H2O	-1.305	0.215
PE	R	-0.413	0.802

Table 5. Results of two-sided student's t-test with 999 Monte Carlo permutations on weighted UniFrac distance matrix for analysis of beta-diversity of eukaryotic community composition between substrate type.

C. Fungi

Boxplots of distance comparisons used for analysis are not included, but were generated in the same manner as for bacterial and eukaryotic, using the weighted Unifrac distance matrix for fungal communities (Appendix 1, **Table D**). Beta-diversity analysis of fungal communities resulted in significant variation (p-values < 0.05) between polymer-associated and free-floating communities for PS, PP, and PE substrate biofilms. Significant values are denoted with an (*) on the table below. No significant differences between communities on different polymer substrates was found. Rubber was not included in fungal analysis as isolation of fungal communities from rubber was not successful.

Group 1	Group 2	T-statistic	Non-parametric p-value
PS	PP	0.554	0.586
PS	PET	-0.019	0.991
PS	H2O	-2.146	*0.04
PS	PE	0.674	0.513
PP	PS	0.499	0.638
PP	PET	-0.322	0.727
PP	H2O	-2.146	*0.033
PP	PE	0.550	0.595
PET	PS	-0.935	0.381
PET	PET	-1.265	0.209
PET	H2O	-1.688	0.104
PET	PE	-1.227	0.245
PE	PS	-0.742	0.471
PE	PP	-0.649	0.522
PE	H2O	-3.870	*0.001
PE	PET	-1.754	0.073

Table 6. Results of two-sided student's t-test with 999 Monte Carlo permutations on Weighted UniFrac distance matrix for analysis of beta-diversity of fungal microbial community composition.

Scanning Electron Microscopy

The following images (**Figures 16-20**) show the surface of polymer samples under a scanning electron microscope. Originally the images were planned for use to quantitatively measure surface degradation, but the number of comparable images and the nature of the degradation proved incompatible with meaningful quantification.

The first two images presented illustrate degradation of the polymer surfaces over time in the sea. **Figure 16**(a) depicts the surface a polyethylene pellet, stored in the laboratory during the six month immersion period; **Figure 16**(b) shows the surface of another PE pellet, this one after immersion for six months. There is a clear increase in surface irregularity from **Image 16**(a) to **Image 16**(b); the same difference in irregularity was observed in all qualitative comparisons of pre and post-immersion samples. Under increased magnification, evaluation of post-immersion polyethylene pellet surfaces show that some irregularity is consistent with organismal growth, while other is filamentous or non-specific degradation of the surface material.

Select images of organismal growth on sample surfaces have also been included for illustrative purposes (**Figures 17-20**).

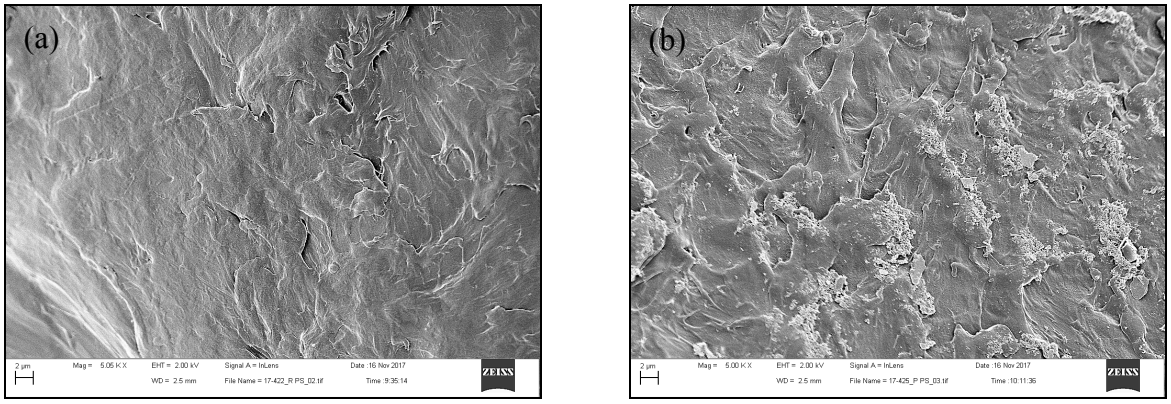

Figure 16. (a) Before and (b) after six month immersion images of the surface of polyethylene pellets. Images were taken at the same magnification (Mag=5Kx) and from the same distance (WD=2.5mm).

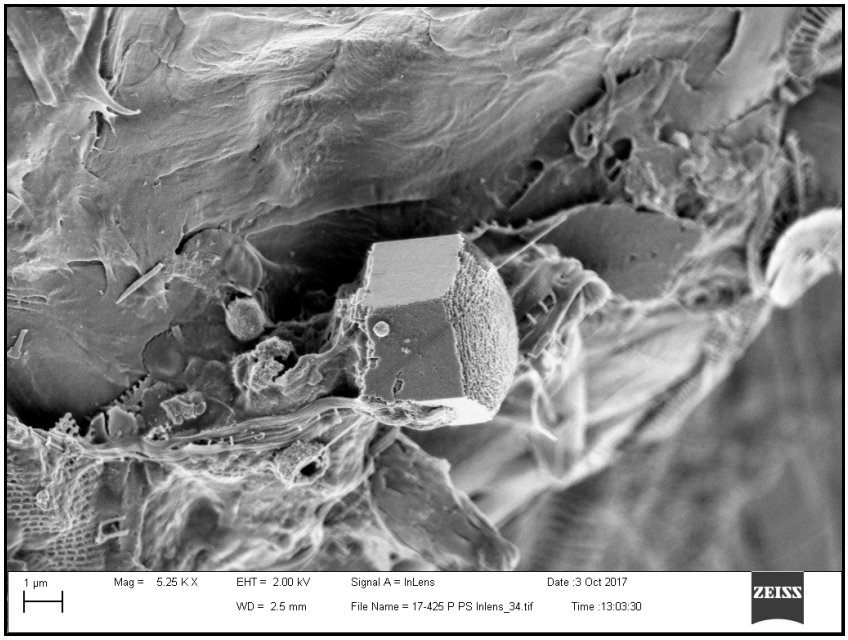

Figure 17. Unknown organism growing on the surface of a polystyrene pellet at six months post-immersion.

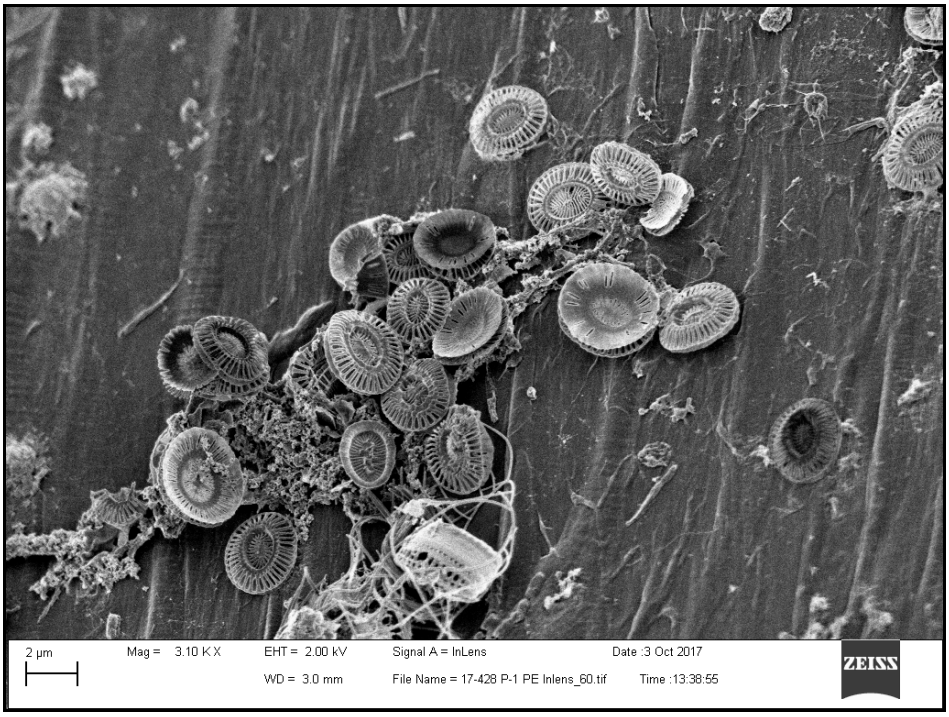

Figure 18. Abundant growth of unidentified diatoms on the surface of a polyethylene sample.

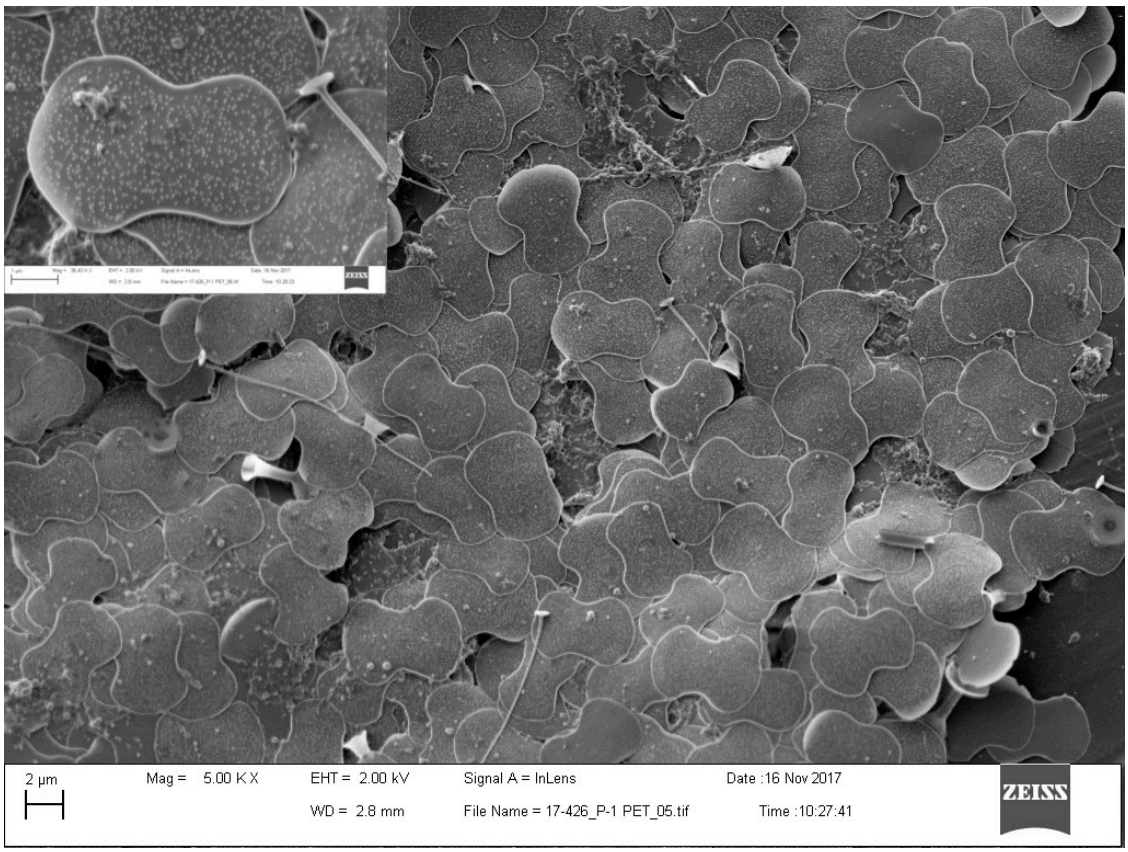

Figure 19. Mat-like growth of microbial biofilm on PET surface, including an up-close view of one of the organisms (in-set photo). Both measuring bars are 2 µm in length.

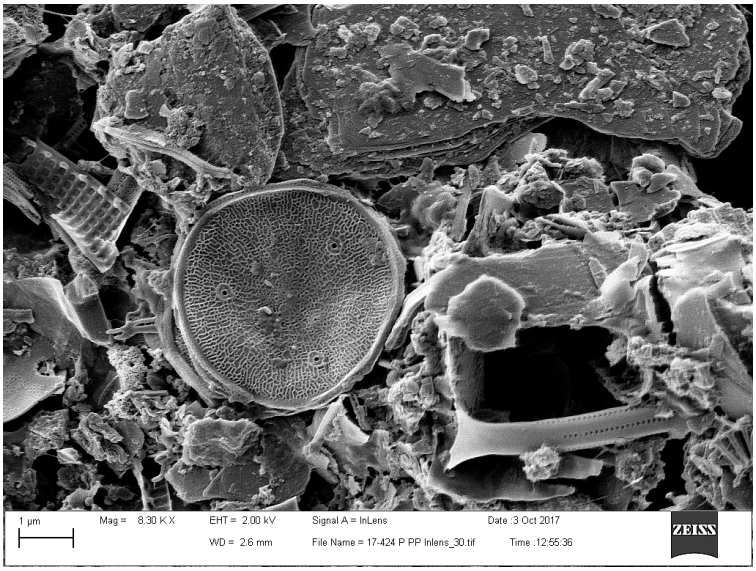

Figure 20. Organism of class Diatomea, possibly *Bacillariophytina* or *Coscinodiscophytina,* growing on a polypropylene pellet sample surface.

Discussion

Temperature and light effects

Temperature results for the duration of the experiment are included in **Figure 7** and, excluding the month of November 2016, provide a comprehensive view of the temperature fluctuations that the samples encountered over the course of the experiment in the Tromsø area. Because many of the previous studies to investigate the marine plastic microbiome were conducted in more temperate climates (Elifantz et al., 2013; Zettler et al., 2013; Oberbeckmann et al., 2016), differences in the community structure between this study and others are likely. As temperature mediates both abiotic and biotic polymer degradation processes, it is an important metric of environmental influence in this study.

Light intensity was recorded for a short period of the experiment before the sensor failed. This could have been due to low water temperature causing a battery failure. Light data was recorded for the period of December 2, 2016 – January 24, 2017, after which time the sensor stopped recording. As this period was during the polar night, the data that was recorded does not provide much insight and was not included in the results. As previously mentioned, most degradation of plastics in the environment is initiated by ultraviolet radiation from the sun (Andrady, 2011). The temporal trend of UV exposure of marine plastic debris in the Arctic likely significantly alters the photo-initiated degradation process, and this may affect the biodegradation of plastic in the Arctic may also proceed differently. Due to the limited success of DNA extraction from samples incubated over the winter, this study is unable to compare community structure between seasons. Future studies could include a comparative analysis of the plastic microbiome in the Arctic in winter versus summer.

Method development: Biofilm removal and DNA extraction

Determining the optimal method for biofilm removal and DNA extraction was an essential step in the sampling process, without which there would be no additional data. Because a straightforward method for biofilm removal and subsequent processing was not immediately clear for the matrix and substrates used in this experiment, several trials were employed.

The initial obstacle was the removal of the biofilm from the plastics, and was the limiting factor in the first trials with winter season samples. Several attempts using a variety of centrifugation steps for biofilm removal, and the MoBio kit for extraction yielded little to no DNA in the extract, while control samples were running at normal yields. This led to the assumption that either biofilm was not being successfully removed by the methods in use, or there was little to no microbial growth during the polar night. Contradictory on-going research at UiT to the latter led to the belief that the barrier to successful isolation of DNA was in the removal of the biofilm itself. Attempts at using variations of buffer solutions, incubations, and centrifugation speeds were repeated failures.

One trial from the winter season was successful at isolating a small amount of DNA. These first measures of DNA resulted from a removal technique using a combination of incubation at 15°C and ribolyzation for 30 seconds x 2. Sample "PET-2-DR10" exhibits the highest DNA concentration, and differed from the others in that it was ribolyzed twice for 1 minute each. This seemed to clarify the need for a mechanical step in the biofilm removal process, however, it still did not provide sufficient DNA concentrations for amplification and sequencing.

After additional research and side-by-side trials with kit extraction vs. enzymatic digestion and phenol-chloroform separation, a new protocol was developed for the summer season samples. The process outlined in the Materials and Methods section for Trial #2 was adapted from a combination of two significant sources (Oberbeckmann et al., 2016; Wright et al., 2009), and basic research in to DNA extraction techniques. In the final process, the plastic pellets were left in the solution during all digestions and incubations, and were only removed prior to phenol-chloroform separation. Additionally, the first incubation in lysis buffer on a shaker at 15°C for one hour proved to be an essential step for presumably loosening the biofilm, enabling the downstream enzymatic digestions to proceed as anticipated. Final concentrations of DNA from Trial #2 samples were sufficient for PCR amplification and downstream sequencing.

Later trials on winter season samples using the new technique yielded higher, though not comparable DNA concentrations, but were not available for sequencing. This could indicate that microbial growth on polymers is lower during the polar night, as might be expected due to the low temperatures and lack of sunlight. It could also be the result of DNA degradation over time,

as the samples were kept frozen at -80°C for a period of 8-10 months before being subject to the new protocol.

Sample size vs. data resolution

In selecting how to best analyze the diversity among and between microbial communities, a choice between sample size and data resolution had to be made. The decision was made to preserve sample size over data resolution, and the resulting data proved sufficient for diversity comparisons as evidenced in the following sections. Further discussion on the reasoning behind this, as well as the study design errors that could have been corrected for, are provided to enhance the results.

At the median rarefaction level, many substrates had one or zero representative samples with a sufficient sequence count, and thus were not valid for comparison of community diversity. Though rarefaction of the sequence data was an assumed part of the analysis, ideally the original sample size would be large enough to analyze at a higher rarefaction level, exclude samples with insufficient data, and still maintain a robust sampling size. By using rarefaction plots to select for the point where the number of species began to level off, it was possible to include nearly all of the samples in the diversity analysis. When comparing analyses between rarefaction levels, differences were minimal, indicating that the lower sequencing depth successfully captured the species distribution.

Though as a whole the sample size was limited by the cost of sequencing, some additional modifications could have been made to correct these sampling issues within the confines of the project. By limiting the number of metrics of comparison, group sample size could have been increased. For example, reducing the type of polymers analyzed to one or two as opposed to five would have increased the sample size for each substrate. Further, biofilm samples from plastics could have been analyzed as a whole instead of broken down by polymer type. Though analysis of substrate specificity was an original goal of this study, at the limited size of this project, it may have proved more useful to prioritize other goals.

Alpha-diversity: insights and notable OTUs

Several hundred OTUs were identified in most biofilm extracts, and a complete analysis of each would be impractical. Here are outlined some of the notable communities as evidenced by their relative abundance, association with plastic-degrading microorganisms, or other notable properties.

a. Location variation

Variation in the Chao 1 alpha diversity index in eukaryotic and fungal communities was observed between samples at Location 1 versus Location 2. Both the Observed Species and Chao 1 metrics for bacterial communities were also nearly significant between samples varied by location. As described in Materials & Methods section pages 18-20, these locations varied in surrounding environments, boat traffic and tidal exposure. As the Chao 1 metric uses both the abundance and evenness of species distribution to calculate a diversity metric, overall these results suggest that samples at Location 1 were colonized by a more diverse group of organisms than those at Location 2. Though the abundance of uncontrolled factors limits the conclusions that can be drawn from this, the tidal shifts experienced at Location 2 seem a likely candidate for explaining this variation. Samples at this location were periodically submerged in seawater and fully exposed to the air, meaning that organisms growing on these samples would also have to be adaptable to the shifting environment.

b. Bacterial OTUs

Overall, polymer-associated biofilms were dominated by a diverse set of bacterial families as evidenced in **Figure 9**. Many of these families (*Rhodobacteraceae, Alteromonadaceae, Flavobacteraceae, Saprospiraceae*) are commonly found surface-associated marine bacteria, involved in the biogeochemical carbon cycle in the ocean (McCarren et al., 2010; Oberbeckmann et al., 2016; Zettler et al., 2013). These results are in agreement with other notable studies of the marine plastic microbiome (Oberbeckmann et al., 2016, Zettler et al., 2013), with some variation in prevalence. Another common family, *Plantomycetaceae*, belong to a unique phylum

(*Plantomycetes*) of aquatic bacteria recently found to play a large role in nitrogen fixation in the open ocean (Delmont et al., 2018). Other studies have found them associated with macro-algae (Faria et al., 2017) and plastic debris (Oberbeckmann et al., 2016).

The most abundant family in all of the polymer-substrate biofilm communities was *Rhodobacteraceae*, a commonly identified member of plastic-associated biofilm communities (Elifantz et al., 2013, Oberbeckmann et al., 2016, Zettler et al., 2013; Debroas et al, 2017). A notable member of this family is *Rhodococcus ruber C208* (Orr et al., 2004), a strain that has been reported to degrade polyethylene film (Orr et al., 2004). Of the polymer-associated biofilms, a range of 6.5% (PE-1-2) to 20.55% (PE 2-2) of OTUs were within the *Rhodobacteraceae* family. Abundant OTUs of *Rhodobacteraceae* were also present in seawater and rubber control samples at comparable levels, though interestingly, at the genus level, most of the *Rhodobacteraceae* in seawater were members of the *Roseobacter* clade (NAC11-7 lineage), while prevalence of *Roseobacter* on polymer samples was minimal to non-existent. Most *Rhodobacteraceae* present on polymer samples were unclassified at the genus level.

Two families of the phylum of Bacteriodetes were present within the top 10 most abundant sequences of polymer-associated OTUs, the most prevalent being *Flavobacteriaceae*. Within the family *Flavobacteriaceae*, the genus *Tenacibaculum* contains several species that are pathogenic to marine fish (Suzuki et al., 2001), most notably Tenacibaculum *maritimum*, the causative agent of tenacibaculosis, an ulcerative disease with global significance causing fish mortality and affecting aquaculture production (Avendaño-Herrera et al., 2006). First isolated in Norway in 2016 on fish used to control sea lice in salmon farms (Småge et al., 2016), monitoring for *T. maritimum* is an on-going effort for the aquaculture industry. Efforts to determine the role of *Tenacibaculum* sp. in ulcerative disease outbreaks in Norwegian farm-raised salmon (Olsen et al., 2011) have indicated their potential role as the combined or sole agent of pathogenesis. A proposed new species (Tenacibaculum *finnmarkense*) has recently been isolated from skin lesions of an Atlantic salmon in Finnmark, Norway during an epizootic (Småge et al., 2016). The current study isolated 11 different OTUs of the genus *Tenacibaculum*, as members of both free-floating and attached communities. Though the resolution was not high enough to positively identify them at the species level, the possibility exists that marine plastic debris harbors pathogenic bacteria that could be harmful to salmon production in Norway.

Also present in small numbers were several members of two obligate hydrocarbon-degrading species, *Alcanivorax* and *Cycloclasticus* (Chronopoulou et al., 2014). *Alcanivorax* species have been identified at rates of up to 50% in oil cores in mudflats (Coulon et al., 2012) and are well adapted to biofilm formation and oil degradation (Schneiker et al., 2006). Interestingly, sequences of *Alcanivorax* were found only in polymer-associated biofilms, no sequences were identified within free-floating microbial communities. Also present were members of the *Pseudomonas* spp., a groups of marine generalists containing strains thought to play a role in the degradation of hydrocarbons, as evidenced by their high abundance in experimental and environmental oil spills (Chronopoulou et al., 2014; Dubinsky et al., 2013). The metabolic potential of these species and others within their families are interesting prospects for investigating the ability of marine microorganisms to degrade hydrocarbon-based plastics.

c. Eukaryotic OTUs

In general, eukaryotic members of polymer-associated biofilm were evenly distributed between *Alveolata*, *Holozoa*, *Chloroplastida* and *Stramenopiles*. The lack of significance of the diversity metrics for eukaryotes indicates that eukaryotic community composition in the marine environment may be more uniform than that of bacterial communities when considering polymer colonization.

The presence of *Stramenopiles*, primarily the most abundant *Diatomea,* is in accordance with other analyses of marine eukaryotic communities on polymer surface (Carson et al, 2013; Oberbeckmann et al, 2016). Their even distribution across all substrate types in this study indicates that they are a common component in biofilm formation on marine plastics. Many members of the *Diatomea* taxa were evident under SEM, and images are included in Results pages 43-44.

Other commonly identified taxa include *Ciliophora (*mainly *Conthreep)* and *Dinoflagellata,* both members of the *Alveolata* super-phlyum. *Alveolata* members are distinctive in their diverse modes of nutrient acquisition (Leander, 2008), ranging from photoautotrophy to predation on bacteria (Stoecker, 1999).

d. Fungal OTUs

Because the majority of fungal OTUs (>85% on all polymer types) were unclassified beyond the domain level, in-depth analysis of fungal OTUs has not been described here.

Beta-Diversity: significant differences in community structure

As described above, significant variation in bacterial and fungal community structure was identified between biofilms on all polymer types versus free-floating organisms. These results are in agreement with two studies on the plastic microbiome conducted in the North Atlantic (Oberbeckmann et al., 2016; Debroas et al, 2017), as well as a study conducted in 2014 (Dussud et al, 2017) in the Western Mediterranean, and support their conclusions that marine plastics represent a unique environment for marine microbes. Interestingly, biofilm samples obtained in two of these previous studies were dominated by *Cyanobacteria* (Debroas et al, 2017; Dussud et al, 2017), while levels of *Cyanobacteria* in biofilms in this study were less than 2%. This is likely the result of different environmental conditions, and illustrates the need for analysis of polymer-associated biofilms under various conditions. Though a complete analysis of plastic-specific bacteria was not included in this study, these findings represent the differential colonization of polymer surfaces by microbial organisms in a novel environment, and prompt further investigation in to the specificity and the metabolic functions of the polymer-associated microbes in the Arctic.

Variation was also significant between several synthetic polymer biofilms and those growing on rubber, the non-synthetic polymer used as a control. To the best of my knowledge, this is the first study to investigate the microbiome present on rubber samples in the marine environment. The significance of community structure variation between the microbiome on the synthetic polymer versus the natural polymer is an interesting result, and supports the idea that polymer surfaces may provide the opportunity for discriminate colonization over other materials by some species. These findings could result from the significant colonization (>56%) of the rubber sample by a Gammaproteobacteria (order 34P16), not isolated on synthetic polymer samples. This order is not fully described in literature, and warrants further investigation as to the reason for its high prevalence on the rubber substrate. Due to the low sample size of the rubber substrate, any

variability that may exist between rubber biofilm communities cannot be discussed. No variation was observed between communities on different types of synthetic polymers over the course of this study.

Fungal community variation between polymer biofilm and free-floating microbes also warrants additional investigation due to the largely unclassified nature of fungal OTUs in this study and in general. Fungi are an important source of potential polymer biodegraders, as a 2011 study (Russell et al., 2011) isolated several endophytic fungi capable of degrading polyurethane, another type of polymer (not included in this study).

Summary

This study improves upon current methods for removing microbial biofilm from microplastics, and the process could be applied to the analysis of biofilm on microplastics for a variety of environments or different downstream processes. The method development portion of this experiment was extensive and included a variety of lab techniques and innovation.

It also provides an in-depth look at the microbial species diversity on plastics after 6 months at sea under Arctic conditions. Investigation of the microbial community diversity reveals the presence of bacterial families containing known plastic and hydrocarbon degrading species, pathogenic microbes, and many notable OTUs within each taxonomic classification. The 16S amplicon sequencing of bacterial isolates was particularly robust in targeting both the V3 and V4 regions of the 16s rRNA gene, and provides a significant wealth of information for investigating marine and polymer-associated bacteria in the Arctic.

Additionally, beta-diversity analysis shows that variation in community structure between free-floating organisms and polymer-associated communities is likely a characteristic common to all polymer types. The significance of this variation in relation to colonization of other material surfaces is an additional point of consideration. While some significant variation between biofilm communities on synthetic polymers compared to rubber was observed, the analysis was limited in that only one sample of rubber biofilm was available for sequencing. Further studies on additional control materials may shed light on the specificity of colonization of synthetic polymer surfaces.

Substrate-specificity was not investigated in depth in this study. Though differences exist between the microbial colonization of one polymer type versus another, particularly between simple carbon-carbon chain polymers and those with heteroatoms in the backbone (i.e. PE versus PET), the significance of these differences was not immediately attributable to substrate-type. Limiting the substrate types under analysis, refining the study to assess discriminate colonization of one polymer type versus another, and increasing the sample size would provide a better method for investigating this hypothesis.

Another goal of this study was to determine if there is any relationship between microbial life present on marine plastics and degradation over time. While this goal has not been achieved, this research provides a foundational basis for continued investigation into the potential role that microbes play in the degradation process. The anticipated method of using image processing on SEM images to quantify surface degradation over time was insufficient for obtaining meaningful quantification. The images, while of excellent quality, proved too non-specific for algorithmic processing. Further research has revealed that using SEM in combination with another more quantitative approach, such as Differential Scanning Calorimetry (EAG Laboratories, Inc., 2016) on pre and post-immersion samples, or HPLC-MS on *in vitro* samples, would provide a more realistic way of measuring degradation over time. While the images were not used quantitatively, they do show clear qualitative distinctions between pre and post-immersion samples, and are an interesting tool for observing and classifying members of the marine plastic biofilm.

References

AMERICAN CHEMISTRY COUNCIL (ACC). Products & Technologies: Plastics: *https://plastics.americanchemistry.com/How-Plastics-Are-Made/*

ANDRADY, A. 2011. Microplastics in the marine environment. *Marine Pollution Bulletin. 62, pp.1596-1605.*

AUSTIN, H.P., ALLEN, M.D., DONOHOE, B.S., RORRER, N.A., KEARNS, F.L., SILVEIRA, R.L., POLLARD, B.C., DOMINICK, G., DUMAN, R., EL OMARI, K., MYKHAYLYK, V., WAGNER, A., MICHENER, W.E., AMORE, A., SKAF, M.S., CROWLEY, M.F., THORNE, A.W., JOHNSON, C.W., WOODCOCK, H.L., MCGEEHAN, J.E., BECKHAM, G.T. 2018. Characterization and engineering of a plastic-degrading aromatic polyesterase. *PNAS, 115(19), pp.4350-4357*.

AVENDANO-HERRERA, R., TOANZO A.E., MAGARINOS, B. 2006. Tenacibaculosis infection in marine fish caused by *Tenibaculum maritimum:* a review. *Diseases of Aquatic Organisms, 71, pp.255-266.*

AVERY-GAUM, S., O'HARA, P.D., KLEINE, L., BOWES, V., WILSON, L.K., BARRY, K.L. 2012. Northern fulmars as biological monitors of trends of plastic pollution in the eastern North Pacific. *Marine Pollution Bulletin, 64(9), pp.1776-1781.*

AZZARELLO, M.Y., VAN-VLEET, E.S. 1987. Marine birds and plastic pollution. *Marine Ecology, 37, pp.295-303.*

BARNES, D.K.A., GALGANI, F., THOMPSON, R.C., BARLAZ, M. 2009. Accumulation and fragmentation of plastic debris in global environments. *Philosophical Transactions B, The Royal Society Publishing, 364(1526), pp. 1985-1998*.

CARSON, H., NERHEIM, M.S., CARROLL, K.A., ERIKSEN, M. 2013. The plastic-associated microorganisms of the North Pacific Gyre. *Marine Pollution Bulletin. 75 (1-2), pp 126-132*.

CHRONOPOULOU, P.M., SANNI, G.O., SILAS-OLU, D.I., ROELOF VAN DER MEER, J., TIMMIS, K.N., BRUSSARD, C.P.D., MCGENITY, T.J. 2014. Generalist hydrocarbon-degrading bacterial communities in the oil-polluted water column of the North Sea.

COULON, F., CHRONOPOULOU, P.M., FAHY, A., PAISSE, S., GONI-URRIZA, M., PEPERZAK, L., ALVAREZ, L.A., MCKEW, B.A., BRUSSAARD, C.P.D., UNDERWOOD, G.J.C., TIMMIS, K.N., DURAN, R., MCGENITY, T.J. 2012. Central role of dynamic tidal biofilms dominated by aerobic hydrocarbonoclastic bacteria and diatoms in the biodegradation of hydrocarbons in coastal mudflats. *Applied and Environmental Microbiolgy, 78(10), pp.3638-3648.*

COZAR, A., ECHEVARRIA, F., GONZALEZ-GORDILLO, J.I., IRIGOIEN, X., UBEDA, B., HERNANDEZ-LEON, S., PALMA, A.T., NAVARRO, S., GARCIA-DE-LOMAS, J., RUIZ., A., FERNANDEZ-DE-PUELLES, M.L., DUARTE, C.M. 2014. Plastic debris in the open ocean. *Proceedings of the National Academy of Science of the United States of America. 111 (28), pp 10239-10244.*

COZAR, A., MARTI, E., DUARTE, C.M., GARCIA-DE-LOMAS, J., VAN SEBILLE, E., BALLATORE, T.J., EGUILUZ, V.M., GONZALEZ-GORDILLO, I., PEDROTTI, M.L., ECHEVARRIA, F., TROUBLE, R., IRIGOIEN, X. 2017. The Arctic Ocean as a dead end for floating plastics in the North Atlantic Branch of the Thermohaline Circulation. *Science Advances, 3(4).*

DEBROAS, D., MONE, A., TER HALLE, A. 2017 Plastics in the North Atlantic garbage patch: A boat-microbe for hitchhikers and plastic degraders. *Science of the Total Environment. 599-600, pp 1222-1232.*

DELMONT, T.O., QUINCE, C., SHAIBER, A., ESEN, O.C., LEE, S., RAPPE, M.S., MACLELLAN, S.L., LUCKER, S., EREN, E.M. 2018. Nitrogen-fixing populations of Platomycetes and Proteobacteria are abundant in surface ocean metagenomics. *Nature Microbiology, published online June 11, 2018.*
DERRAIK, J.G.B. 2002. The pollution of the marine environment by plastic debris: a review. *Marine Pollution Bulletin, 44(9), pp.842-852.*

DUBINSKY, E.A., CONRAD, M.E., CHAKRABORTL, R., BILL, M., BORGLIN, S.E., HOLLIBAUGH, J.T., MASON, O.U., PICENOT, Y.M., REID, F.C., STRINGFELLOW, W.T., TOM, L.M., HAZEN, T.C., ANDERSEN, G.L. 2013. Succession of hydrocarbon-degrading bacteria in the aftermath of the *Deepwater Horizon* oil spill in the Gulf of Mexico. *Environmental Science & Technology, 47(19), pp.10860-10867.*

DUSSUD, C., MEISTERTZHEIM, A.L., CONAN, P., PUJO-PAY, M., GEORGE, M., FABRE, P., COUDANE, J., HIGGS, P., ELINEAU, A., PEDROTTI, M.L., GORSKY, G., GHIGLIONE, J.F. Evidence of niche partitioning among bacteria living on plastics, organic particles and surrounding seawaters. 2018. *Environmental Pollution, 236, pp. 807-816.*

EAG LABORATORIES, INC. 2016. Characterization of Polymers Using Differential Scanning Calorimetry (DSC). Retrieved from:
https://www.azom.com/article.aspx?ArticleID=15458

ELIFANTZ, H., HORN, G., AYON, M., COHEN, Y., MINZ, D. 2013. *Rhodobacteraceae* are the key members of the microbial community of the initial biofilm formed in Eastern Mediterranean coastal seawater. *FEMS Microbiology Ecology, 85(2), pp.348-357.*
ENGLER, R.E. 2012. The complex interaction between marine debris and toxic chemicals in the ocean. *Environmental Science & Technology. 46(22), pp.12302-12315.*

VAZQUEZ-BAEZA, Y., PIRRUNG M., GONZALEZ A., KNIGHT R. *EMPeror: a tool for visualizing high-throughput microbial community data, Gigascience. 2013 Nov 26;2(1):16.*

FARIA, M., BORDIN, N., KIZINA, J., HARDER, J., DEVOS, D., LAGE, O.M. 2017. *Plantomycetes* attached to algal surfaces: Insight into their genomes. *Genomics.*
GEWART, B., PLASSMANN, M.M., MACLEOD, M. 2015. Pathways for degradation of plastic polymers floating in the marine environment. *Environmental Science: Processes & Impacts, 17, pp.1513-1521.*

HADAD, D., GERESH, S., SIVAN, A. 2005. Biodegradation of polyethylene by the thermophilic bacterium *Brevibacillus borstenlensis*. *Journal of Applied Microbiology, 98(5), pp.1093-1100.*

HAN, X., LIU, W., HUANG, J.W., MA, J., ZHENG, Y., KO, T.P., XU, L., CHENG, Y.S., CHEN, C.C., GUO, R.T. 2017. Structural insight into the catalytic mechanism of PET hydrolase. *Nature Communications, 8(1).*

IHRMARK, K., BÖDEKER I.T.M., CRUZ-MARTINEZ, K., FRIBERG, H., KUBARATOVA, A., SCHENCK, J., STRID, Y., STENLID, J., BRANDSTRÖM-DURLING, M., CLEMMENSEN, K.E., LINDHAL, B.D. 2012. New primers to amplify the fungal ITS2 region – evaluation by 454-seuencing of artificial and natural communities. *FEMS Microbiology Ecology, 82(3), pp.666-677.*

JAMBECK, J.R., GEYER, R., WILCOX, C., SIEGLER, T.R., PERRYMAN, M., ANDRADY, A., NARAYAN, R., LAW, K.L. 2015. Plastic waste inputs from land into the ocean. *Science, 347(6223), pp.768-771.*

KAISER, D., KOWALSKI, N., WANIEK, J. J., 2017. Effects of biofouling on the sinking behavior of microplastics. *Environmental Research Letters. 12 (12).*

KLINDWORTH, A., PRUESSE, E., SCHWEER, T., PEPLIES, J., QUAST, C., HORN, M., GLÖCKNER, F.O. 2013. Evaluation of general 16S ribosomal RNA gene PCR primers for classical and next-generation sequencing-based diversity studies. *Nucleic Acids Research, 41(1), pp.1-11.*

KOSETH, M., MASON, S.A., WATTENBERG, E.V. 2018. Anthropogenic contamination of tap water, beer, and sea salt. *PLOS ONE, April 11, 2018.*
LAVERS, J.L., BOND, A.L. 2017. Exceptional and rapid accumulation of anthropogenic debris on one of the world's most remote and pristine islands. *Proceedings of the National Academy of Sciences of the United States of America (PNAS), 114(23), pp.6052-6055.*

LEANDER, B.S. 2008. Alveolates. Alveolata. Version 16 September 2008. Retrieved from: http://tolweb.org/Alveolates/2379

LOZUPONE, C., KNIGHT, R., 2005. UniFrac: a New Phylogenetic Method for Comparing Microbial Communities. *Applied and Environmental Microbiology. 71 (12), pp 8228 – 8235.*

MARINE DEBRIS: *Understanding, Preventing and Mitigating the Significant Adverse Impacts on Marine and Coastal Biodiversity.* 2016. Technical Series No.83. Secretariat of the Convention on Biological Diversity, Montreal, 78 pages.

MCCARREN, J., BECKER, J.W., REPETA, D.J., SHI, Y., YOUNG, C.R., MALMSTROM, R.R., CHISHOLM, S.W., DELONG, E.F. 2010. Microbial community transcriptomes reveal microbes and metabolic pathways associated with dissolved organic matter turnover in the sea. *PNAS, 107(38), pp.16420-16427*.

MCCARREN, J.; BACKER, J. W.; REPETA, D. J.; SHI Y.; YOUG, C. R.; MALSTROM, R. R.; CHISHOLM, S. W.; DELONG, E. F. Microbial community transcriptomes reveal microbes and metabolic pathways associated with dissolved organic matter turnover in the sea Proc. *Natl. Acad. Sci. U.S.A.* 2010, 107 (38) 16420– 7

MURPHY, F., EWINS, C., CARBONNIER, F., QUINN, B. 2016. Wastewater treatment works (WwTW) as a source of microplastics in the aquatic environment. *Environmental Science & Technology, 50(11), pp.5800-5808*.

NATIONAL OCEANANIC AND ATMOSPHERIC ADMINISTRATION (NOAA) MARINE DEBRIS PROGRAM. 2014. Report on the Entanglement of Marine Species in Marine Debris with an Emphasis on Species in the United States. Silver Spring, MD. *28 pp*

NOAA MARINE DEBRIS PROGRAM. *2015.* Report on the impacts of "ghost fishing" via derelict fishing gear. *Silver Spring, MD. 25 pp.*

NOAA, A GUIDE TO PLASTIC IN THE OCEAN. 2018. *https://oceanservice.noaa.gov/hazards/marinedebris/plastics-in-the-ocean.html*

OBERBECKMANN, S., OSBORN, A.M., DUHAIME, M.B. 2016. Microbes on a bottle: substrate, season and geography influence community composition of microbes colonizing marine plastic debris. *PLoS One. 11(8).*

OLSEN, A., NILSEN, H., SANDLUND, N., COLQUHOUN, D. 2011. Tenacibaculum spp. associated with winter ulcers in sea-reared Atlantic salmon Salmo salar. *Diseases of Aquatic Organisms, 94(3), pp.189-99.*

ORR, I.G., HADAR, Y., SIVAN, A. 2004. Colonization, biofilm formation and biodegradation of polyethylene by a strain of Rhodococcus ruber. *Applied Microbiological Biotechnology, 65(1), PP.97-104*.

PEEKEN, I., PRIMPKE, S., BEYER, B., GUTERMANN, J., KATLEIN, C., KRUMPEN, T., BERGMANN, M., HEHEMANN, L., GERDTS, G. 2018. Arctic sea ice is an important temporal sink and means of transport for microplastic. *Nature Communications. 9:1505.*

PETERSON, J.D., VYAZOKIN, S., WIGHT, C.A. 2001. Kinetics of the thermal and thermo-oxidative degradation of polystyrene, polyethylene and poly(propylene). *Macromolecular Chemistry and Physics. 202(6), pp.775-784.*

PHUONG, N.N., Zalouk-Vergnoux, A., Kamari, A., Mouneyrac, C., Amiard, F., Poirier, L., Lagarde, F. 2018. Quantification and characterization of microplastics in blue mussels (*Mytilus edulis*): protocol setup and preliminary data on the contamination of the French Atlantic coast. *Environmental Science and Pollution Research. 25(7), pp 6135-6144.*

PLASTICSEUROPE: ASSOCIATION OF PLASTIC MANUFACTURERS. 2017. Plastics – the Facts, 2017. *https://www.plasticseurope.org/application/files/5715/1717/4180/Plastics_the_facts_2017_FINAL_for_website_one_page.pdf*

RAUM-SUYURAN, K.L., JEMISON, L.A., PITCHER, K.W. 2009. Entanglement of Stellar sea lions (*Eumetopias jubatus)* in marine debris: Identifying causes and finding solutions. *Marine Pollution Bulletin, 58(10), pp.1487-1495.*

ROCHMAN, C.M., HOH, E., KUROBE, T., THE, S.J. 2013. Ingested plastic transfers hazardous chemicals to fish and induces hepatic stress. *Scientific Reports, 3:3263.*

ROCHMANN, C.M., HUH, E., HENTSCHEL, B.T., KAYE, S. 2013. Long-term field measurement of sorption of organic contaminants to five types of plastic pellets: Implications for plastic marine debris. *Environmental Science & Technology, 47(3), pp.1646-1654.*

RUMMEL, C.D., LODER, M.G.J., FRICKE, N.F., LANG, T., GRIEBLER, E.M., JANKE., M., GERDTS, G. 2016. Plastic ingestion by pelagic and demersal fish from the North Sea and Baltic Sea. *Marine Pollution Bulletin, 102(1), pp.134-141.*

RUSSELL, J.R., HUANG, J., ANAND, P., KUCERA, K., SANDOVAL, A.G., DANTZLER, K.W., HICKMAN, D., LEE, J., KIMOVEC, F.M., KOPPSTEIN, D., MARKS, D.H., MITTERMILLER, P.A., NUNEZ S.J., SANTIAGO, M., TOWNES, M.A., VISHEVETSKY, M., WILLIAMS, N.E., VARGAS, M.P.N., BOULANGER, L.A., BASCOM-SLACK, C., STROBEL, S.A. 2013. Biodegradation of polyester polyurethane by endophytic fungi. *Applied and Environmental Microbiology, 77(17), pp.6076-6084.*

SCHMIDT, C., KRAUTH, T., WAGNER, S. 2017. Export of plastic debris by rivers in to the sea. *Environmental Science & Technology. 51, pp.12246-12253.*

SCHNEIKER, S., MARTIN DOS SANTOS, V.A.P., BARTELS, D., BEKEL, T., BRECHT, M, BUHRMESTER, J., CHERNIKOVA, T.N., DENARO, R., FERRER, M., GERTLER, C., GOESSMANN, A., GOLYSHINA, O.V., KAMINSKI, F., KHACHANE, A.N., LANG, S., LINKE, B., MCHARDY, A.C., MEYER, F., NECHITAYLO, T., PUHLER, A., REGENHARDT, D., RUPP, O., SABIROVA, J.S., SELBITSCHKA, W., YAKIMOV, M.M., TIMMIS, K.N., VORHOLTER, F.J., WEIDNER, S., KAISER, O., GOLYSHIN, P.N.

2006. Genome sequence of the ubiquitous hydrocarbon-degrading marine bacterium *Alcanivorax borkumensis*. *Nature Biotechnology, 25, pp.997-1004*.

SMAGE, S.B., FRISCH, K., BREVIK, O., WATANABE, K., NYLUND, A. 2016. First isolation, identification and characterization of *Tenibaculum maritimum* in Norway, isolated from diseased farmed sea lice cleaner fish *Cyclopterus lumpus* L. *Aquaculture, 464, pp.178-184.*

SMAGE, S.B., FRISCH, K., BREVIK, O., WATANABE, K., NYLUND, A. 2016. *Tenibaculum finnmarkense* sp. nov., a fish pathogenic bacterium of the family *Flavobacteriaceae* isolated from Atlantic salmon.

STOECK, T., BASS, D., NEBEL, M., CHRISTEN, R., JONES, M.D., BREINER, H.W,. RICHARDS, T.A. 2010. Multiple marker parallel tag environmental DNA sequencing reveals a highly complex eukaryotic community in marine anoxic water. *Molecular Ecology, 19, pp.21-31.*

STOECKER, D.K. 1999. Mixotrophy among dinoflagellates. *Journal of Eukaryotic Microbiology. 46, pp 397-401.*

SUZUKI, M., NAKAGAWA, Y., HARAYAMA, S., YAMAMOTO, S. 2001. Phylogenetic analysis and taxonomic study of marine Cytophaga-like bacteria: proposal for Tenacibaculum gen. nov. with Tenacibaculum maritimum comb. nov. and Tenacibaculum ovolyticum comb. nov., and description of Tenacibaculum mesophilium sp. nov. and Tenacibaculum amulolyticum sp. nov. *International Jounral of Systematic and Evolutionary Microbiology, 51, pp.1639-1652.*

TANAKA, K., TAKADA, H., YAMASHITA, R., MIZUKAWA, K., FUKUWAKA, M., WATANUKI, Y. 2013. Accumulation of plastic-derived chemicals in tissues of seabirds ingesting marine plastics. *Marine Pollution Bulletin, 69(1,2), pp.219-222.*

TEUTEN, E.L., SAQUING, J.M., KNAPPE, D., BARLAZ, M.A., JONSSON, S., BJORN, A., ROWLAND, S.J., THOMPSON, R.C., GALLOWAY, T.S., YAMASHITA, R., OCHI, D., WATANUKI, Y., ZAKARIA, M.P., AKKHAVONG, K., OGATA, Y., HIRAI, H., IWASA, S., MIZUKAWA, K., HAGINO, Y., IMAMURA, A., SAHA, M., TAKADA, H. 2009. Transport and release of chemicals from plastics to the environment and to wildlife. *Philosophical Transactions of the Royal Society B, 364(1526).*

WALSH, D.A., ZAIKOVA, E., HALLAM, S.J. 2009. Small volume (1-3 L) filtration of coastal seawater samples. *Journal of Visualized Experiments: JoVE, 28, 1163.*

WEI, R., OESER, T., ZIMMERMAN, W. 2014. Chapter Seven – Synthetic polyester-hydrolyzing enzymes from thermophilic actinomycetes. *Advances in Applied Microbiology, 89, pp.267-305.*

WILCOX, C., VAN SEBILLE, E., HARDESTY, B.D. 2015. Threat of plastic pollution to seabirds is global, pervasive, and increasing. *PNAS. 112(38), pp.11899-11904.*

WORLD ECONOMIC FORUM, ELLEN MACARTHUR FOUNDATION AND MCKINSEY & COMPANY. 2016. *The New Plastics Economy: Rethinking the future of plastics:* http://www.ellenmacarthurfoundation.org/publications

WORLDWATCH INSTITUTE, 2015. Global plastic production rises, recycling lags. Vital Signs: *Global Trends That Shape Our Future: vitalsigns.wordwatch.org*.

WRIGHT, J.J., LEE, S., ZAIKOVA, E., WALSH, D.A., HALLAM, S.J. 2009. DNA Extraction from 0.22µm Sterivex filters and cesium chloride density gradient centrifugation. *Jounral of Visualized Experiments: JoVE, 31, 1352.*

YOSHIDA, S., HIRAGA, K., TAKEHANA, T., TANIGUCHI, I., YAMAJI, H., MAEDA, Y., TOYOHARA, K., MIYAMOTO, K., KIMURA, Y., ODA, K. 2016. A bacterium that degrades and assimilates poly(ethylene terephthalate). *Science, 351(6278), pp.1196-1199*.

ZETTLER, E.R., MINCER, T.J., AMARAL-ZETTLER, L.A. 2013. Life in the "Plastisphere": Microbial communities on plastic marine debris. *Environmental Science & Technology, 47, pp.7137-7146.*

Appendix 1

The following table contains inline-barcodes and sample IDs used by LGC Genomics for in-house tracking:

Sample	Inline barcode
341F-785R-16S-16S-DR10	NACAACTGTGT
341F-785R-16S-16S-H2O1-1	NAACAGCTCAT
341F-785R-16S-16S-H2O1-3	NNACTGTTGACT
341F-785R-16S-16S-H2O2-1	NNNAGAGTTGCTT
341F-785R-16S-16S-H2O2-3	ACCTTGACAT
341F-785R-16S-16S-PE1-1	NNNAAGTCTTCGT
341F-785R-16S-16S-PE1-2	NNACAAGGTCTT
341F-785R-16S-16S-PE2-1	NNAGTCATCCTT
341F-785R-16S-16S-PE2-2	NNNAGTAGCCTAT
341F-785R-16S-16S-PET1-2	NAACAGACCTT
341F-785R-16S-16S-PET1-3	ACAACCAGTT
341F-785R-16S-16S-PET2-1	NNACTTAGCACT
341F-785R-16S-16S-PET2-2	NNNAATACGACCT
341F-785R-16S-16S-PET2-3	ACGATCGTAT
341F-785R-16S-16S-PP1-1	NNNAATGCGCTAT
341F-785R-16S-16S-PP1-2	NNACGATACGTT
341F-785R-16S-16S-PP2-1	NACCAATCAGT
341F-785R-16S-16S-PP2-2	NNAGGACTTGTT
341F-785R-16S-16S-PP2-3	NNNAGCTGAATCT
341F-785R-16S-16S-PS1-2	NAAGCTCACTT
341F-785R-16S-16S-PS1-3	ACATGAGGTT
341F-785R-16S-16S-PS2-1	ACTCACTGTT
341F-785R-16S-16S-PS2-2	NAGAGCAATGT
341F-785R-16S-16S-PS2-3	AGATAGCGAT
341F-785R-16S-16S-R1-1	ACCTCATCTT
Eu565F-Eu981R-18S-18S-DR10	NAGAGCAATGT
Eu565F-Eu981R-18S-18S-H2O1-1	NACCAATCAGT
Eu565F-Eu981R-18S-18S-H2O1-3	NNAGGACTTGTT
Eu565F-Eu981R-18S-18S-H2O2-1	NNNAGCTGAATCT
Eu565F-Eu981R-18S-18S-H2O2-3	ACTCACTGTT

Eu565F-Eu981R-18S-18S-PE1-1	NNNAGAGTTGCTT
Eu565F-Eu981R-18S-18S-PE1-2	NNACTGTTGACT
Eu565F-Eu981R-18S-18S-PE2-1	NNATGCGCATAT
Eu565F-Eu981R-18S-18S-PE2-2	NNNAGTGCTTCAT
Eu565F-Eu981R-18S-18S-PET1-2	NAACAGCTCAT
Eu565F-Eu981R-18S-18S-PET1-3	ACCTCATCTT
Eu565F-Eu981R-18S-18S-PET2-1	NNAGTCATCCTT
Eu565F-Eu981R-18S-18S-PET2-2	NNNAGTAGCCTAT
Eu565F-Eu981R-18S-18S-PET2-3	ACTGAAGGAT
Eu565F-Eu981R-18S-18S-PP1-1	NNNAATACGACCT
Eu565F-Eu981R-18S-18S-PP1-2	NNACTTAGCACT
Eu565F-Eu981R-18S-18S-PP2-1	NAACGGAACAT
Eu565F-Eu981R-18S-18S-PP2-2	NNATATAGCCGT
Eu565F-Eu981R-18S-18S-PP2-3	NNNAGTGAACTCT
Eu565F-Eu981R-18S-18S-PS1-2	NACAACTGTGT
Eu565F-Eu981R-18S-18S-PS1-3	ACCTTGACAT
Eu565F-Eu981R-18S-18S-PS2-1	ATACGGACTT
Eu565F-Eu981R-18S-18S-PS2-2	NAGCTCCTTAT
Eu565F-Eu981R-18S-18S-PS2-3	ACAACCAGTT
Eu565F-Eu981R-18S-18S-R1-1	ACGATCGTAT
ITS7F-ITS4R-ITS2-ITS-DR10	NACGTCACT
ITS7F-ITS4R-ITS2-ITS-H2O1-1	NACGATCAT
ITS7F-ITS4R-ITS2-ITS-H2O1-3	NNACGCATAT
ITS7F-ITS4R-ITS2-ITS-H2O2-1	NNNACGTACAT
ITS7F-ITS4R-ITS2-ITS-H2O2-3	ACGTATCT
ITS7F-ITS4R-ITS2-ITS-PE1-1	NNNACAGATCT
ITS7F-ITS4R-ITS2-ITS-PE1-2	NNACACTGAT
ITS7F-ITS4R-ITS2-ITS-PE2-1	NNACTATCGT
ITS7F-ITS4R-ITS2-ITS-PE2-2	NNNACTATGCT
ITS7F-ITS4R-ITS2-ITS-PET1-2	NACACTAGT
ITS7F-ITS4R-ITS2-ITS-PET1-3	ACACGTAT
ITS7F-ITS4R-ITS2-ITS-PET2-1	NNACGTCTGT
ITS7F-ITS4R-ITS2-ITS-PET2-2	NNNACGTGAGT
ITS7F-ITS4R-ITS2-ITS-PET2-3	ACGTGTAT
ITS7F-ITS4R-ITS2-ITS-PP1-1	NNNACATACGT
ITS7F-ITS4R-ITS2-ITS-PP1-2	NNACAGTCAT

ITS7F-ITS4R-ITS2-ITS-PP2-1	NACTACAGT
ITS7F-ITS4R-ITS2-ITS-PP2-2	NNACTACGAT
ITS7F-ITS4R-ITS2-ITS-PP2-3	NNNACTAGACT
ITS7F-ITS4R-ITS2-ITS-PS1-2	NACAGTACT
ITS7F-ITS4R-ITS2-ITS-PS1-3	ACAGCTAT
ITS7F-ITS4R-ITS2-ITS-PS2-1	ACTAGCAT
ITS7F-ITS4R-ITS2-ITS-PS2-2	NACTAGTGT
ITS7F-ITS4R-ITS2-ITS-PS2-3	ACTGTAGT
ITS7F-ITS4R-ITS2-ITS-R1-1	ACGATACT

Table A. Sample identification chart used by LGC Genomics for in-house sample tracking during the amplification and sequencing procedures. Inline barcodes were attached to the 5' end of the forward and reverse primers, and were used for identification post-demultiplexing.

The following weighted Unifrac tables contain the distance measurements used for diversity calculations as referenced in the results section on beta-diversity analysis.

	16S-16S-H	16S-16S-P	16S-16S-H	16S-16S-P	16S-16S-P	16S-16S-P	16S-16S-P	16S-16S-R	16S-16S-P	16S-16S-P	16S-16S-P	16S-16S-P	16S-16S-P	16S-16S-P
16S-16S-H	0.00	0.49	0.09	0.55	0.55	0.60	0.44	0.72	0.45	0.49	0.53	0.55	0.45	0.57
16S-16S-P	0.49	0.00	0.49	0.53	0.54	0.59	0.21	0.78	0.17	0.23	0.26	0.54	0.43	0.54
16S-16S-H	0.09	0.49	0.00	0.55	0.57	0.61	0.45	0.74	0.46	0.49	0.53	0.56	0.46	0.58
16S-16S-P	0.55	0.53	0.55	0.00	0.23	0.25	0.48	0.63	0.46	0.45	0.43	0.18	0.22	0.15
16S-16S-P	0.55	0.54	0.57	0.23	0.00	0.15	0.48	0.52	0.46	0.47	0.46	0.17	0.24	0.22
16S-16S-P	0.60	0.59	0.61	0.25	0.15	0.00	0.53	0.51	0.50	0.51	0.50	0.20	0.29	0.25
16S-16S-P	0.44	0.21	0.45	0.48	0.48	0.53	0.00	0.73	0.13	0.20	0.23	0.48	0.37	0.49
16S-16S-R	0.72	0.78	0.74	0.63	0.52	0.51	0.73	0.00	0.72	0.74	0.74	0.58	0.62	0.64
16S-16S-P	0.45	0.17	0.46	0.46	0.46	0.50	0.13	0.72	0.00	0.20	0.21	0.46	0.35	0.47
16S-16S-P	0.49	0.23	0.49	0.45	0.47	0.51	0.20	0.74	0.20	0.00	0.14	0.46	0.36	0.44
16S-16S-P	0.53	0.26	0.53	0.43	0.46	0.50	0.23	0.74	0.21	0.14	0.00	0.45	0.35	0.43
16S-16S-P	0.55	0.54	0.56	0.18	0.17	0.20	0.48	0.58	0.46	0.46	0.45	0.00	0.22	0.18
16S-16S-P	0.45	0.43	0.46	0.22	0.24	0.29	0.37	0.62	0.35	0.36	0.35	0.22	0.00	0.24
16S-16S-P	0.57	0.54	0.58	0.15	0.22	0.25	0.49	0.64	0.47	0.44	0.43	0.18	0.24	0.00
16S-16S-H	0.39	0.61	0.42	0.59	0.53	0.54	0.53	0.58	0.54	0.58	0.58	0.55	0.51	0.61
16S-16S-P	0.56	0.54	0.56	0.17	0.22	0.24	0.49	0.61	0.47	0.45	0.44	0.17	0.23	0.18
16S-16S-H	0.37	0.55	0.39	0.62	0.56	0.57	0.49	0.64	0.50	0.54	0.58	0.58	0.52	0.65
16S-16S-P	0.48	0.15	0.48	0.52	0.53	0.58	0.20	0.77	0.18	0.25	0.25	0.53	0.42	0.53
16S-16S-P	0.48	0.20	0.49	0.51	0.50	0.55	0.20	0.72	0.17	0.27	0.25	0.50	0.39	0.51
16S-16S-P	0.47	0.18	0.47	0.47	0.47	0.52	0.20	0.72	0.14	0.24	0.23	0.48	0.37	0.49
16S-16S-P	0.51	0.50	0.52	0.15	0.20	0.24	0.43	0.60	0.42	0.42	0.40	0.16	0.18	0.18

Table B. Weighted Unifrac distance matrix used for diversity analysis of bacterial communities, based on 16S amplicon phylogenies.

	18S-18S-P	18S-18S-P	18S-18S-P	18S-18S-P	18S-18S-R	18S-18S-P	18S-18S-P	18S-18S-P	18S-18S-P	18S-18S-H	18S-18S-H	18S-18S-P	18S-18S-P
18S-18S-P	0.00	0.46	0.91	0.68	0.90	0.27	0.30	1.11	0.86	0.92	0.98	0.99	0.94
18S-18S-P	0.46	0.00	0.94	0.68	1.01	0.44	0.47	1.14	0.80	0.92	1.01	0.99	0.95
18S-18S-P	0.91	0.94	0.00	0.67	0.82	0.95	0.96	0.85	0.84	0.66	0.61	0.99	0.92
18S-18S-P	0.68	0.68	0.67	0.00	0.80	0.69	0.69	0.94	0.66	0.61	0.72	0.83	0.75
18S-18S-R	0.90	1.01	0.82	0.80	0.00	1.06	1.08	0.87	0.67	0.88	0.91	0.78	0.74
18S-18S-P	0.27	0.44	0.95	0.69	1.06	0.00	0.12	1.17	0.84	0.92	1.00	1.01	0.98
18S-18S-P	0.30	0.47	0.96	0.69	1.08	0.12	0.00	1.19	0.87	0.94	1.02	1.03	1.00
18S-18S-P	1.11	1.14	0.85	0.94	0.87	1.17	1.19	0.00	0.81	1.01	1.01	1.01	0.96
18S-18S-P	0.86	0.80	0.84	0.66	0.67	0.84	0.87	0.81	0.00	0.79	0.89	0.49	0.42
18S-18S-H	0.92	0.92	0.66	0.61	0.88	0.92	0.94	1.01	0.79	0.00	0.27	0.97	0.86
18S-18S-H	0.98	1.01	0.61	0.72	0.91	1.00	1.02	1.01	0.89	0.27	0.00	1.04	0.94
18S-18S-P	0.99	0.99	0.99	0.83	0.78	1.01	1.03	1.01	0.49	0.97	1.04	0.00	0.29
18S-18S-P	0.94	0.95	0.92	0.75	0.74	0.98	1.00	0.96	0.42	0.86	0.94	0.29	0.00
18S-18S-H	1.00	1.02	0.66	0.78	0.86	1.02	1.03	0.97	0.83	0.49	0.49	0.97	0.90
18S-18S-H	1.03	1.06	0.61	0.84	0.88	1.05	1.07	0.97	0.88	0.55	0.46	1.02	0.94
18S-18S-P	0.97	0.99	0.72	0.73	0.75	0.99	1.01	0.91	0.48	0.66	0.75	0.51	0.43
18S-18S-P	1.08	1.09	0.98	0.84	0.84	1.10	1.11	0.81	0.53	0.94	1.00	0.51	0.44
18S-18S-P	0.86	0.80	0.80	0.59	0.70	0.85	0.87	0.77	0.31	0.75	0.84	0.62	0.54
18S-18S-P	1.11	1.10	1.02	0.88	0.89	1.09	1.09	1.04	0.63	0.99	1.05	0.31	0.38
18S-18S-P	0.18	0.49	0.84	0.61	0.90	0.29	0.30	1.09	0.83	0.89	0.95	0.94	0.89
18S-18S-P	0.68	0.65	0.71	0.56	0.78	0.68	0.71	0.98	0.68	0.77	0.85	0.90	0.86
18S-18S-P	0.34	0.44	0.85	0.60	0.87	0.46	0.49	1.09	0.79	0.88	0.97	0.96	0.92

Table C. Weighted Unifrac distance matrix used for beta-diversity analysis of eukaryotic (18S amplicon) microbial communities.

	ITS2-ITS-P	ITS2-ITS-P	ITS2-ITS-P	ITS2-ITS-H	ITS2-ITS-H	ITS2-ITS-P	ITS2-ITS-P	ITS2-ITS-P	ITS2-ITS-P	ITS2-ITS-P	ITS2-ITS-P	ITS2-ITS-P	ITS2-ITS-P
ITS2-ITS-P	0.00	0.43	0.42	2.49	2.32	2.59	2.16	0.74	2.60	2.40	0.25	0.46	0.81
ITS2-ITS-P	0.43	0.00	0.37	2.57	2.40	2.69	2.25	0.70	2.69	2.47	0.36	0.70	0.76
ITS2-ITS-P	0.42	0.37	0.00	2.39	2.21	2.53	2.03	0.65	2.58	2.32	0.38	0.65	0.61
ITS2-ITS-H	2.49	2.57	2.39	0.00	0.61	1.87	1.75	2.60	1.93	1.79	2.50	2.44	2.28
ITS2-ITS-H	2.32	2.40	2.21	0.61	0.00	1.93	1.59	2.40	2.00	1.84	2.33	2.27	2.15
ITS2-ITS-P	2.59	2.69	2.53	1.87	1.93	0.00	1.33	2.70	1.14	1.14	2.60	2.52	2.44
ITS2-ITS-P	2.16	2.25	2.03	1.75	1.59	1.33	0.00	2.19	1.37	1.16	2.17	2.09	2.08
ITS2-ITS-P	0.74	0.70	0.65	2.60	2.40	2.70	2.19	0.00	2.71	2.46	0.66	0.97	1.07
ITS2-ITS-P	2.60	2.69	2.58	1.93	2.00	1.14	1.37	2.71	0.00	0.99	2.63	2.50	2.54
ITS2-ITS-P	2.40	2.47	2.32	1.79	1.84	1.14	1.16	2.46	0.99	0.00	2.40	2.35	2.36
ITS2-ITS-P	0.25	0.36	0.38	2.50	2.33	2.60	2.17	0.66	2.63	2.40	0.00	0.50	0.79
ITS2-ITS-P	0.46	0.70	0.65	2.44	2.27	2.52	2.09	0.97	2.50	2.35	0.50	0.00	0.82
ITS2-ITS-P	0.81	0.76	0.61	2.28	2.15	2.44	2.08	1.07	2.54	2.36	0.79	0.82	0.00
ITS2-ITS-H	2.89	2.97	2.83	1.47	1.60	1.82	2.04	3.00	1.85	1.96	2.90	2.84	2.73
ITS2-ITS-P	1.64	1.73	1.54	2.05	1.84	1.70	1.12	1.62	1.70	1.41	1.66	1.60	1.63
ITS2-ITS-P	1.86	1.94	1.72	1.83	1.64	1.45	0.96	1.85	1.40	1.21	1.87	1.77	1.77
ITS2-ITS-P	0.89	0.79	0.79	2.62	2.43	2.72	2.25	0.32	2.73	2.50	0.83	1.11	1.18
ITS2-ITS-H	2.47	2.55	2.38	1.21	1.11	1.78	1.56	2.55	1.92	1.78	2.47	2.41	2.31
ITS2-ITS-P	1.66	1.55	1.47	1.84	1.70	2.13	1.78	1.76	2.22	2.06	1.65	1.66	1.10
ITS2-ITS-P	1.68	1.57	1.50	1.63	1.52	2.01	1.66	1.79	2.11	1.97	1.66	1.67	1.27
ITS2-ITS-P	2.51	2.56	2.43	1.81	1.89	0.72	1.28	2.60	1.09	1.12	2.51	2.48	2.36
ITS2-ITS-P	2.30	2.36	2.18	1.55	1.58	1.09	1.09	2.37	1.02	0.98	2.28	2.23	2.12

Table D. Weighted Unifrac distance matrix used for beta-diversity analysis of fungal (ITS amplicon) communities.